O.E.C.D. HIGH TEMPERATURE REACTOR PROJECT

DRAGON

**Dragon Project Report**

# THE COMPARISON OF CARBON-ATOM DISPLACEMENT RATE IN GRAPHITE IN THE DRAGON REACTOR, THE PETTEN HTR AND LOW ENRICHMENT HTR

by

D. L. REED

A.E.E. Winfrith, Dorchester, Dorset, England

May, 1967

# THE COMPARISON OF CARBON-ATOM DISPLACEMENT RATE IN GRAPHITE IN THE DRAGON REACTOR, THE PETTEN HFR AND A LOW ENRICHMENT HTR

by

D. L. REED

ABSTRACT

This report describes the way in which the physical behaviour of graphite irradiated in different reactors can be related to one another by using a common fast neutron dose scale. The dose scale used is achieved by converting the measured nickel or iron fast neutron dose to an equivalent fission dose (or fluence). A relationship is established between the carbon atom displacement rate and the equivalent fission flux. Using high energy neutron spectra calculated by a Monte Carlo method the carbon atom displacement rate per unit equivalent fission flux in DRAGON and the Petten HFR were respectively 1.51 and 1.75 times that in PLUTO (or DIDO).

With the same methods of fast neutron spectrum calculation in a typical low enrichment HTR with a power density of 8 $MW/m^3$ it was found that the time required to reach a DIDO nickel dose of $2 \times 10^{22}$ n $cm^{-2}$ in the graphite moderator immediately adjacent to the fuel was 15.4 years. In addition the carbon atom displacement rate per unit equivalent fission flux in the moderator was found to vary between 1.46 and 2.26 times that in PLUTO (or DIDO).

## CONTENTS


| | | PAGE NO. |
|---|---|---|
| 1. | INTRODUCTION | 5 |
| | PART I | |
| 2. | A COMPARISON OF CARBON-ATOM DISPLACEMENT RATES IN GRAPHITE IN THE DRAGON REACTOR AND THE PETTEN HFR | 5 |
| | 2.1 Theory | 5 |
| | 2.2 Data Used in the Calculations | 8 |
| | 2.3 Calculation of the Neutron Spectra using the Monte Carlo Method | 8 |
| | 2.4 Details of the Calculations | 12 |
| | 2.5 Discussion of the Results | 13 |
| | PART II | |
| 3. | CALCULATION OF FAST FLUX AND CARBON ATOM DISPLACEMENT RATE IN A LOW ENRICHMENT HTR | 13 |
| | 3.1 Introduction | 13 |
| | 3.2 Details of the Calculations | 20 |
| | 3.3 Discussion | 22 |
| 4. | CONCLUSIONS | 22 |
| 5. | ACKNOWLEDGMENT | 24 |
| 6. | REFERENCES | 24 |


## LIST OF TABLES


| TABLE | | |
|---|---|---|
| 1. | Ni-58 (n,p) Co-58 Cross Section | 9 |
| 2. | Fe-54 (n,p) Mn-54 Cross Section | 10 |
| 3. | The Thompson-Wright Carbon Damage Function | 10 |
| 4. | Carbon Scattering Cross Section | 11 |
| 5. | Group Structure of Neutron Spectra | 12 |

| TABLE | | PAGE NO. |
|---|---|---|
| 6. | Average Cross Sections for the Core of the First Charge of Dragon | 14 |
| 7. | Average Cross Sections for the Uprated U,Zr Element in Dragon | 15 |
| 8. | Average Cross Sections in the First Dragon Capsule in Position E7 of the Petten HFR Core 243 | 16 |
| 9. | Average Cross Sections in Region of Element D7 in Petten HFR Core 243 | 17 |
| 10. | Average Cross Sections in the Second Dragon Capsule in Position E8 of the 30 MW Petten HFR Core | 18 |
| 11. | Carbon-Atom Displacement Rate in Units of $10^{-24}$ Atoms/Atom Normalised to Unit Equivalent Fission Flux | 19 |
| 12. | Material Composition of Cell Regions | 20 |
| 13. | Boundaries of Regions in the Cell | 21 |
| 14. | Results of the Calculations in a Cell of a Low Enrichment HTR | 23 |


## LIST OF ILLUSTRATIONS


FIGURE

1. The DRAGON Fuel Element
2. Cross Section of a DRAGON Capsule in the Petten HFR
3. Cross Section of the HFR Core 243
4. Cross Section of the 30 MW HFR Petten
5. Sections through the DRAGON Reactor showing Regions in which Neutron Spectra were Calculated
6. Regions in which Spectra Calculations were Performed on the Uprated U,Zr Element in DRAGON
7. Regions in which Spectra Calculations were Performed in E7 of the HFR Core 243
8. Regions in which Spectra Calculations were Performed in D5 of the HFR Core 243
9. Regions in which Spectra Calculations were Performed in E8 of the 30 MW HFR Core
10. High Energy Spectrum in a Thorium Element at the Centre of the First DRAGON Core

FIGURE

11. High Energy Spectrum in the Central Fuel Rod of the DRAGON Uprated U,Zr Element

12. High Energy Spectrum in the Outer Six Fuel Rods of the DRAGON Uprated U,Zr Element

13. High Energy Spectrum in the First DRAGON Capsule in the Petten HFR

14. High Energy Spectrum in D5 of the Petten HFR Core 243

15. High Energy Spectrum in the Second DRAGON Capsule in the Petten HFR

16. The DIDO Nickel Dose in a Cell of a Low Enrichment HTR

17. The Number of Years Required to Reach an Equivalent DIDO Nickel Dose of $2 \times 10^{22}$ in a cell of a Low Enrichment HTR

# THE COMPARISON OF CARBON-ATOM DISPLACEMENT RATE IN GRAPHITE IN THE DRAGON REACTOR, THE PETTEN HFR AND A LOW ENRICHMENT HTR

by

D. L. REED

## 1. INTRODUCTION

Graphite samples have been irradiated in both the DRAGON Reactor and the Petten HFR, and nickel and cobalt monitors have been used in both reactors to measure the fast neutron dose (or fluence). The correlation of the irradiation results and their application to power reactor designs requires that a common dose-scale be adopted. Fortunately a relationship can be established between the nickel dose and displacement rate of carbon atoms in graphite provided that the nickel dose is normalised in the correct way for each activation. The normalisation essentially consists in correcting the displacement rate to that which would occur in an equivalent fission spectrum. This is necessary since the Ni-58 (n,p) Co-58 reaction has a threshold of approximately 3 MeV, whilst carbon atom displacement occur at energies of ca. 70 keV and upwards. Thus the measured nickel dose is markedly dependent on the shape of the neutron spectrum which is in turn dependent on the environment. For this reason detailed neutron spectrum calculations between 10 keV and 14 MeV have been performed using the Monte Carlo technique for both reactors in order to correct for the differences in the Ni-58 (n,p) Co-58 reaction rate. So far only the effects of the neutron spectra have been taken into account but the correlation of physical changes in graphite due to irradiations in different reactors also depends on the dose rate. The dose rate effect is not considered in this report since it can only be adequately accounted for by experiment.

In the second part of the report a direct application of the Monte Carlo method was made to calculate the fast neutron spectra in a cell of a typical low enrichment HTR. In addition fast flux levels have been calculated and an estimate made of the time taken to reach a DIDO nickel dose of $2 \times 10^{22}$ n cm$^{-2}$ is given. These calculations place the chosen reactor design on the same dose scale as the experimental data and so assist in the evaluation of various aspects of the core design.

## PART I

## 2. A COMPARISON OF CARBON-ATOM DISPLACEMENT RATES IN GRAPHITE IN THE DRAGON REACTOR AND THE PETTEN HFR

### 2.1 Theory

The relationship between the displacement rate of carbon atom and fast neutron dose in graphite will now be established. In the following analysis only the nickel monitor is considered but identical expressions between displacement rate of carbon atoms in graphite and fast neutron dose can be derived for an iron monitor. Measurements of fast neutron

flux by a threshold detector are expressed as equivalent fission fluxes [1] defined by:

$$\phi_{\text{fission}}(\text{Ni}) = \frac{\int_{10\ \text{keV}}^{14\ \text{MeV}} \sigma(\text{Ni})\ \phi\ dE}{\hat{\sigma}(\text{Ni})} \qquad (1)$$

where:

$\sigma(\text{Ni})$ = Ni-58 (n,p) Co-58 cross section for nickel

and

$$\hat{\sigma}(\text{Ni}) = \frac{\int_{0}^{\infty} \sigma(\text{Ni})\ \Phi\ dE}{\int_{0}^{\infty} \Phi\ dE} \qquad (2)$$

where:

$\Phi$ = Neutron flux from primary fissions in the energy interval E to E + dE.

$\phi$ = Neutron flux in a reactor in the energy interval E and E + dE.

Let an average nickel cross section in the reactor be defined by:

$$\overline{\sigma}(\text{Ni}) = \frac{\int_{10\ \text{keV}}^{14\ \text{MeV}} \sigma(\text{Ni})\ \phi\ dE}{\int_{10\ \text{keV}}^{14\ \text{MeV}} \phi\ dE} \qquad (3)$$

Hence equations (1) and (3) give

$$\int_{10\ \text{keV}}^{14\ \text{MeV}} \phi\ dE = \frac{\hat{\sigma}(\text{Ni})}{\overline{\sigma}(\text{Ni})}\ \phi_{\text{fission}}(\text{Ni}) \qquad (4)$$

Let us now define a carbon atom displacement cross section $\sigma_D(E)$ for graphite as a product of the total scattering cross section $\sigma_S(E)$ and the number of displacements of carbon atoms $\nu(E)$, i.e.

$$\sigma_D(E) = \nu(E)\, \sigma_S(E) \tag{5}$$

Hence the rate of displacement of carbon atoms in a reactor between 10 keV and 14 MeV is given by D where:

$$D = \int_{10\ keV}^{14\ MeV} \sigma_D(E)\, \phi(E)\, dE \tag{6}$$

Using equation (4) the displacement rate can be written as

$$D = \bar{\sigma}_D \frac{\hat{\sigma}(Ni)}{\bar{\sigma}(Ni)} \phi_{fission}(Ni) \tag{7}$$

where:

$$\bar{\sigma}_D = \frac{\int_{10\ keV}^{14\ MeV} \sigma_D(E)\, \phi(E)\, dE}{\int_{10\ keV}^{14\ MeV} \phi(E)\, dE}$$

From equation (7) the total number of displacements of carbon atoms after time t is given by:

$$Dt = \bar{\sigma}_D \frac{\hat{\sigma}(Ni)}{\bar{\sigma}(Ni)} \phi_{fission}(Ni)t \tag{8}$$

Equation (8) gives the required relationship between the displacement of atoms in graphite due to fast neutrons and the experimental neutron dose using nickel as a monitor since $\phi_{fission}(Ni)t$ is the equivalent fission dose or fluence for a nickel monitor. To compare the displacement rate of carbon atoms in graphite from one reactor to another it is therefore necessary to convert measurements of the equivalent fission fluence using a nickel fast flux monitor to the number of carbon atom displacements by multiplying by the factor $\bar{\sigma}_D \frac{\hat{\sigma}(Ni)}{\bar{\sigma}(Ni)}$. This has been carried out for a number of different fuel elements in DRAGON and in the Dragon capsules in the Petten HFR.

## 2.2 Data Used in the Calculations

The cross section data used for the Fe-54 (n,p) Mn-54 and Ni-58 (n,p) Co-58 reactions were supplied by Dr. S. Wright and are reported in [2]. Using these data Carter [2] found that $\hat{\sigma}$ for Ni-58 (n,p) Co-58 and Fe-54 (n,p) Mn-54 was 108 and 77 mb respectively for the Cranberg fission spectrum [3], the experimental data from [3] of 107 and 77 mb were however used in this report to be consistent with the analysis of the dose measurements. The rate of displacement of carbon atoms was calculated from the Thompson-Wright damage function for graphite [4] and the total scattering cross section for carbon from the Winfrith and Aldermaston Nuclear Data Library [5]. These data are given in Tables 1 to 4.

## 2.3 Calculation of the Neutron Spectra using the Monte Carlo Method

The Monte Carlo method adopted was specific [6] which is a modified version of Specific [7]. There were three reasons for using this method to calculate the high energy neutron spectra:

(1) to take into account the heterogeneity of the Petten HFR core, in particular the effect of the water moderator,

(2) to compare directly with the calculation of S. B. Wright [4] of $\bar{\sigma}_D \left(\frac{\hat{\sigma}(Ni)}{\bar{\sigma}(Ni)}\right)$ for other reactors using the same data and method of calculation,

(3) to enable neutron spectra to be calculated very near to or within the source of fast neutrons which are not achieved in the required detail by neutron transport or diffusion theory.

Specific is designed to estimate fluxes in a three dimensional rectangular cell which must have at least one square cross section. The cell may be divided into regions whose boundaries are cylinders centred on the middle of the square, and planes at right angles to these. At the outer boundaries neutrons can escape, be totally or partially reflected into the cell by means of an albedo factor. For the neutron source regions independent but similar to the material regions a source strength of uniform density is specified. The energies of the source neutrons are chosen from the Cranberg fission spectrum [3] between 0.05 and 5.97 MeV, above and below these energies empirical formulae describing the spectrum are used. To reduce time in tracking neutrons a splitting technique called "Russian Roulette" is used to concentrate the neutrons into regions of interest and reduce the length of time spent in the other regions.

The neutron spectra in each region are calculated using the total neutron track length scored as a function of neutron energy. This method of scoring enables neutron spectra to be calculated for voids or regions of very low density. To prevent large scatter in the track length scores in a void region a maximum track length value of 30 cm is introduced into the programme so that if a track length of a neutron exceeds this value

T

Table 1

Ni-58 (n,p) Co-58 Cross Section

| E MeV | σ mb | E MeV | σ mb | E MeV | σ mb |
|---|---|---|---|---|---|
| 0.1400 02 | 0.8084 03 | 0.1395 02 | 0.3570 03 | 0.1341 02 | 0.4000 03 |
| 0.1288 02 | 0.4400 03 | 0.1238 02 | 0.4780 03 | 0.1189 02 | 0.5150 03 |
| 0.1142 02 | 0.5480 03 | 0.1098 02 | 0.5770 03 | 0.1055 02 | 0.6020 03 |
| 0.1013 02 | 0.6250 03 | 0.9735 01 | 0.6400 03 | 0.9353 01 | 0.6530 03 |
| 0.8987 01 | 0.6630 03 | 0.8634 01 | 0.6680 03 | 0.8296 01 | 0.6700 03 |
| 0.7970 01 | 0.6690 03 | 0.7658 01 | 0.6660 03 | 0.7358 01 | 0.6600 03 |
| 0.7069 01 | 0.6520 03 | 0.6792 01 | 0.6440 03 | 0.6526 01 | 0.6330 03 |
| 0.6270 01 | 0.6220 03 | 0.6024 01 | 0.6110 03 | 0.5788 01 | 0.5970 03 |
| 0.5561 01 | 0.5830 03 | 0.5343 01 | 0.5680 03 | 0.5133 01 | 0.5510 03 |
| 0.4932 01 | 0.5330 03 | 0.4739 01 | 0.5150 03 | 0.4553 01 | 0.4950 03 |
| 0.4374 01 | 0.4740 03 | 0.4203 01 | 0.4500 03 | 0.4038 01 | 0.4230 03 |
| 0.3880 01 | 0.4000 03 | 0.3727 01 | 0.3620 03 | 0.3581 01 | 0.3270 03 |
| 0.3441 01 | 0.2930 03 | 0.3306 01 | 0.2620 03 | 0.3176 01 | 0.2350 03 |
| 0.3052 01 | 0.2100 03 | 0.2932 01 | 0.1850 03 | 0.2817 01 | 0.1660 03 |
| 0.2707 01 | 0.1470 03 | 0.2601 01 | 0.1290 03 | 0.2499 01 | 0.1110 03 |
| 0.2401 01 | 0.9800 02 | 0.2307 01 | 0.8400 02 | 0.2216 01 | 0.7100 02 |
| 0.2129 01 | 0.6000 02 | 0.2046 01 | 0.5200 02 | | |

T

Table 2

Fe-54 (n,p) Mn-54 Cross Section

| E MeV | σ mb | E MeV | σ mb | E MeV | σ mb |
|---|---|---|---|---|---|
| 0.1585 02 | 0.2770 03 | 0.1555 02 | 0.2921 03 | 0.1525 02 | 0.3077 03 |
| 0.1495 02 | 0.3236 03 | 0.1465 02 | 0.3399 03 | 0.1435 02 | 0.3563 03 |
| 0.1405 02 | 0.3728 03 | 0.1375 02 | 0.3892 03 | 0.1345 02 | 0.4056 03 |
| 0.1315 02 | 0.4217 03 | 0.1285 02 | 0.4375 03 | 0.1255 02 | 0.4529 03 |
| 0.1225 02 | 0.4677 03 | 0.1195 02 | 0.4820 03 | 0.1165 02 | 0.4955 03 |
| 0.1135 02 | 0.5082 03 | 0.1105 02 | 0.5200 03 | 0.1075 02 | 0.5308 03 |
| 0.1045 02 | 0.5404 03 | 0.1015 02 | 0.5488 03 | 0.9850 01 | 0.5559 03 |
| 0.9550 01 | 0.5616 03 | 0.9250 01 | 0.5658 03 | 0.8950 01 | 0.5683 03 |
| 0.8650 01 | 0.5692 03 | 0.8350 01 | 0.5682 03 | 0.8050 01 | 0.5653 03 |
| 0.7750 01 | 0.5603 03 | 0.7450 01 | 0.5533 03 | 0.7150 01 | 0.5440 03 |
| 0.6850 01 | 0.5325 03 | 0.6550 01 | 0.5185 03 | 0.6250 01 | 0.5019 03 |
| 0.5950 01 | 0.4828 03 | 0.5650 01 | 0.4609 03 | 0.5350 01 | 0.4363 03 |
| 0.5050 01 | 0.4087 03 | 0.4750 01 | 0.3781 03 | 0.4450 01 | 0.3443 03 |
| 0.4150 01 | 0.3074 03 | 0.3850 01 | 0.2671 03 | 0.3550 01 | 0.2235 03 |
| 0.3250 01 | 0.1763 03 | 0.2950 01 | 0.1254 03 | 0.2650 01 | 0.7091 02 |
| 0.2350 01 | 0.1256 02 | | | | |

T

Table 3

The Thompson-Wright Carbon Damage Function

| E MeV | ν | E MeV | ν | E MeV | ν |
|---|---|---|---|---|---|
| 14.0 | 547.4 | 8.986 | 510.2 | 6.024 | 476.6 |
| 4.038 | 441.8 | 3.306 | 423.6 | 2.707 | 404.4 |
| 1.814 | 363.0 | 1.216 | 320.4 | 0.815 | 279.0 |
| 0.546 | 231.8 | 0.366 | 189.8 | 0.246 | 151.0 |
| 0.165 | 115.0 | 0.110 | 83.2 | 0.740-01 | 60.0 |
| 0.496-01 | 42.2 | 0.332-01 | 29.6 | 0.223-01 | 21.0 |
| 0.149-01 | 14.4 | 0.100-01 | 10.0 | 0.100-03 | 0.1 |

T

Table 4

Carbon Scattering Cross Section

| E MeV | σ barns | E MeV | σ barns | E MeV | σ barns |
|---|---|---|---|---|---|
| 14.0 | 1.35 | 13.41 | 1.33 | 12.88 | 1.30 |
| 12.37 | 1.28 | 11.89 | 1.25 | 11.42 | 1.22 |
| 10.97 | 1.19 | 10.55 | 1.06 | 10.13 | 1.04 |
| 9.735 | 1.03 | 9.353 | 1.03 | 8.987 | 1.05 |
| 8.634 | 1.20 | 8.296 | 1.34 | 7.97 | 1.50 |
| 7.658 | 1.68 | 7.358 | 1.77 | 7.069 | 0.87 |
| 6.792 | 0.87 | 6.526 | 1.26 | 6.270 | 1.49 |
| 6.024 | 1.07 | 5.788 | 1.08 | 5.561 | 1.21 |
| 5.343 | 1.20 | 5.133 | 1.15 | 4.932 | 1.20 |
| 4.739 | 1.29 | 4.553 | 1.56 | 4.374 | 1.90 |
| 4.203 | 1.94 | 4.038 | 1.87 | 3.880 | 2.05 |
| 3.727 | 2.16 | 3.581 | 2.26 | 3.441 | 2.29 |
| 3.306 | 2.05 | 3.176 | 1.16 | 3.052 | 2.20 |
| 2.932 | 2.82 | 2.817 | 1.90 | 2.706 | 1.68 |
| 2.601 | 1.62 | 2.499 | 1.57 | 2.401 | 1.56 |
| 2.307 | 1.59 | 2.216 | 1.61 | 2.129 | 2.20 |
| 2.046 | 1.70 | 1.965 | 1.78 | 1.888 | 1.83 |
| 1.814 | 1.88 | 1.743 | 1.93 | 1.675 | 1.98 |
| 1.609 | 2.03 | 1.546 | 2.07 | 1.485 | 2.12 |
| 1.427 | 2.17 | 1.371 | 2.22 | 1.318 | 2.28 |
| 1.266 | 2.33 | 1.216 | 2.38 | 1.168 | 2.44 |
| 1.123 | 2.48 | 1.079 | 2.54 | 1.036 | 2.59 |
| 0.9957 | 2.64 | 0.9567 | 2.69 | 0.9192 | 2.74 |
| 0.8831 | 2.80 | 0.8485 | 2.84 | 0.8152 | 2.90 |
| 0.7833 | 2.94 | 0.7526 | 2.99 | 0.7231 | 3.04 |
| 0.6947 | 3.09 | 0.6675 | 3.14 | 0.6413 | 3.18 |
| 0.6161 | 3.23 | 0.5920 | 3.27 | 0.5688 | 3.32 |
| 0.5465 | 3.36 | 0.5250 | 3.40 | 0.5045 | 3.44 |
| 0.4847 | 3.48 | 0.4657 | 3.53 | 0.4474 | 3.57 |
| 0.3122 | 3.93 | 0.2359 | 4.16 | 0.1859 | 4.30 |
| 0.106 | 4.46 | 0.6055-01 | 4.55 | 0.4397-01 | 4.66 |
| 0.9617-02 | 4.76 | 0.001 | 4.76 | | |

Note that $0.5121\text{-}01 = 0.5121 \times 10^{-1}$

$0.5121\ 01 = 0.5121 \times 10^{1}$

no score is recorded. For the types of reactor considered this track length cut-off has been found not to distort the spectra [1].

Since the computed fluxes depend on the source strength all the spectra have been normalised to a source strength within the cell of $10^4$ n/s.

## 2.4 Details of the Calculations

Irradiation of graphite samples has been carried out in the central thorium region of the DRAGON first charge core [8] and also in capsules at the boundary between the core and the reflector of the Petten HFR [9]. In the case of DRAGON the graphite samples were placed in the spines of the fuel rods as shown in Fig. 1, and in the case of Petten HFR the graphite samples were placed in a graphite cylinder (or capsule) which replaced a beryllium reflector element, Fig. 2.

Calculations of spectra were performed for the following cases:

(1) In the central thorium region (N = 10) in the core of the first charge of DRAGON.

(2) In an uprated uranium/zirconium element placed in the centre of the DRAGON core as in case (1).

(3) The DRAGON capsule in position E7 of the Petten HFR Core 243 the details of which are shown in Fig. 3.

(4) In position D5 of Petten HFR Core 243.

(5) The DRAGON capsule in position E8 of the 30 MW Petten HFR core, the details of which are shown in Fig. 4.

The details of the regions in which the spectrum calculations were performed for each case are shown in Figs. 5, 6, 7, 8 and 9. In all these calculations the fission source for each region was either deduced from thermal flux measurements or where these measurements were not available from calculated thermal fluxes. The group structure of the calculated spectrum is given in Table 5 below.

Table 5
Group Structure of Neutron Spectra

| Energy Range MeV | No. of Equal Lethargy Groups |
|---|---|
| 0.01- 0.1 | 5 |
| 0.1 - 1.0 | 40 |
| 1.0 -10.0 | 20 |
| 10.0 -14.0 | 10 |

For each case the average cross sections $\bar{\sigma}$ (n,p), $\bar{\sigma}$ (n,p) and $\bar{\sigma}_D$ were calculated together with $\bar{\sigma}_D \left(\frac{\hat{\sigma}(Ni)}{\bar{\sigma}(Ni)}\right)$ in every region and are given in Tables 6, 7, 8, 9 and 10. The neutrons were concentrated into regions of interest using the "Splitting Technique" previously described in order to improve the accuracy of the spectra and finally of the computed average cross sections.

Ni-58 Fe-54

## 2.5 Discussion of the Results

In order to compare one case with another it was decided to consider average cross sections in only those regions in the central plane of the reactor core in question, since these were the regions in which the concentration of neutrons was greatest. The neutron spectra associated with these regions for each case are shown in Figs. 10, 11, 12, 13, 14 and 15. Table 11 lists the values of $\bar{\sigma}_D \left(\frac{\hat{\sigma}(Ni)}{\bar{\sigma}(Ni)}\right)$ for each case in the region of interest, the spread in this quantity due to the statistical error in the neutron spectra is not greater than 5%. In addition the second column in Table 11 gives the comparison of $\bar{\sigma}_D \left(\frac{\hat{\sigma}(Ni)}{\bar{\sigma}(Ni)}\right)$ with that for the Empty Lattice Position in PLUTO [4].

The application of this particular Monte Carlo programme SPECIFIC to calculations of high energy neutron spectra at a reflector core interface of the Petten HFR is of course questionable since there are considerable changes in the flux gradient with position in these regions of the reactor. In the case of DRAGON the calculations are not in doubt since they were made for the central region of the core. Since there is an element of doubt in the validity of these calculations it has been decided to make an experimental calibration which will give the ratio of the damage fluxes in the Petten HFR to that in BEPO or PLUTO.

The two most important results of the calculations given in Table 11 are that the carbon atom displacement rate in graphite normalised to unit fission flux in the DRAGON reactor and in the first DRAGON capsule in the Petten HFR are respectively 1.51 and 1.75 to that in PLUTO (or DIDO). Recent results [8, 9] from the measurement of graphite shrinkage in the Petten HFR and DRAGON tend to confirm these ratios and so support the validity of the Monte Carlo calculations.

# PART II

# 3. CALCULATION OF FAST FLUX AND CARBON ATOM DISPLACEMENT RATE IN A LOW ENRICHMENT HTR

## 3.1 Introduction

A natural extension to the work described in Part I was to calculate the carbon-atom displacement rate in current designs of High Temperature Power Reactors. One of the main points to be answered in power reactors with graphite moderators is the length of time it will take to reach a

T

Table 6

Average Cross Sections for the Core of the First Charge of Dragon

| Region | $\bar{\sigma}_D$ [4] $10^{-24}$ atoms/atom | $\bar{\sigma}$(Ni) mb | $\bar{\sigma}$(Fe) mb | $\bar{\sigma}_D \left(\frac{\hat{\sigma}(Ni)}{\bar{\sigma}(Ni)}\right)$ [4] $10^{-24}$ atoms/atom | $\left(\frac{\hat{\sigma}(Fe)}{\bar{\sigma}(Fe)}\right) / \left(\frac{\hat{\sigma}(Ni)}{\bar{\sigma}(Ni)}\right)$ |
|---|---|---|---|---|---|
| 1 | 473 | 12.06 | 7.145 | 4,197 | 1.2145 |
| 2 | 493 | 13.27 | 8.201 | 3,978 | 1.1644 |
| 3 | 537 | 29.05 | 17.722 | 1,980 | 1.1796 |
| 4 | 519 | 24.41 | 14.790 | 2,276 | 1.1877 |
| 5 | 542 | 29.72 | 18.462 | 1,953 | 1.1584 |
| 6 | 529 | 26.43 | 16.431 | 2,143 | 1.1576 |
| 7 | 549 | 28.58 | 17.581 | 2,056 | 1.1698 |
| 8 | 532 | 24.98 | 15.216 | 2,279 | 1.1814 |
| 9 | 481 | 14.87 | 8.796 | 3,458 | 1.2166 |
| 10 | 486 | 13.65 | 8.101 | 3,810 | 1.2126 |

T

Table 7

Average Cross Sections for the Uprated U,Zr Element in Dragon

| Region | $\bar{\sigma}_D$ [4] $10^{-24}$ atoms/atom | $\bar{\sigma}_{Ni}$ mb | $\bar{\sigma}_{Fe}$ mb | $\bar{\sigma}_D \left(\frac{\bar{\sigma}(Ni)}{\bar{\sigma}(Ni)}\right)$ [4] $10^{-24}$ atoms/atom | $\left(\frac{\bar{\sigma}(Fe)}{\bar{\sigma}(Fe)}\right) / \left(\frac{\bar{\sigma}(Ni)}{\bar{\sigma}(Ni)}\right)$ |
|---|---|---|---|---|---|
| 1 | 485 | 13.988 | 7.580 | 3,712 | 1.3280 |
| 2 | 489 | 21.499 | 13.512 | 2,432 | 1.1450 |
| 3 | 451 | 16.276 | 10.018 | 2,962 | 1.1691 |
| 4 | 576 | 40.998 | 18.519 | 1,503 | 1.5931 |
| 5 | 546 | 31.699 | 19.794 | 1,844 | 1.1524 |
| 6 | 524 | 26.847 | 16.862 | 2,090 | 1.1457 |
| 7 | 562 | 35.626 | 22.309 | 1,687 | 1.1492 |
| 8 | 539 | 28.390 | 17.686 | 2,031 | 1.1552 |
| 9 | 527 | 24.641 | 15.287 | 2,286 | 1.1600 |
| 10 | 577 | 38.794 | 23.813 | 1,592 | 1.1724 |
| 11 | 543 | 30.755 | 19.116 | 1,887 | 1.1578 |
| 12 | 529 | 27.471 | 17.560 | 2,059 | 1.1258 |
| 13 | 518 | 12.578 | 7.199 | 4,411 | 1.2574 |
| 14 | 518 | 20.627 | 13.715 | 2,685 | 1.0823 |
| 15 | 531 | 13.923 | 7.064 | 4,081 | 1.4185 |

T

Table 8

Average Cross Sections in the First Dragon Capsule in Position E7 of the Petten HFR Core 243

| Region | $\bar{\sigma}_D$ [4] $10^{-24}$ atoms/atom | $\bar{\sigma}_{Ni}$ mb | $\bar{\sigma}_{Fe}$ mb | $\bar{\sigma}_D \left(\frac{\hat{\sigma}(Ni)}{\bar{\sigma}(Ni)}\right)$ [4] $10^{-24}$ atoms/atom | $\left(\frac{\hat{\sigma}(Fe)}{\bar{\sigma}(Fe)}\right) / \left(\frac{\hat{\sigma}(Ni)}{\bar{\sigma}(Ni)}\right)$ |
|---|---|---|---|---|---|
| 1 | 551 | 29.918 | 18.069 | 1,972 | 1.1916 |
| 2 | 569 | 29.055 | 17.709 | 2,094 | 1.1807 |
| 3 | 569 | 28.021 | 16.761 | 2,174 | 1.2031 |
| 4 | 554 | 26.109 | 15.664 | 2,270 | 1.1995 |
| 5 | 568 | 28.129 | 17.038 | 2,160 | 1.1881 |
| 6 | 561 | 24.400 | 14.623 | 2,462 | 1.2007 |
| 7 | 527 | 24.199 | 14.648 | 2,331 | 1.1888 |
| 8 | 542 | 29.664 | 17.965 | 1,957 | 1.1883 |
| 9 | 548 | 24.904 | 14.647 | 2,355 | 1.2236 |

T

Table 9

Average Cross Sections in Region of Element D5 in Petten HFR Core 243

| Region | $\bar{\sigma}_D$ [4] $10^{-24}$ atoms/atom | $\bar{\sigma}_{Ni}$ mb | $\bar{\sigma}_{Fe}$ mb | $\bar{\sigma}_D \left(\frac{\hat{\sigma}(Ni)}{\bar{\sigma}(Ni)}\right)$ [4] $10^{-24}$ atoms/atom | $\left(\frac{\hat{\sigma}(Fe)}{\bar{\sigma}(Fe)}\right) / \left(\frac{\hat{\sigma}(Ni)}{\bar{\sigma}(Ni)}\right)$ |
|---|---|---|---|---|---|
| 1 | 620 | 38.024 | 22.917 | 1,745 | 1.1940 |
| 2 | 626 | 41.629 | 25.450 | 1,610 | 1.1771 |
| 3 | 622 | 39.794 | 24.304 | 1,672 | 1.1783 |
| 4 | 611 | 37.990 | 23.427 | 1,721 | 1.1670 |
| 5 | 617 | 39.551 | 24.320 | 1,669 | 1.1703 |
| 6 | 612 | 36.440 | 21.933 | 1,797 | 1.1956 |
| 7 | 607 | 35.767 | 22.214 | 1,815 | 1.1587 |
| 8 | 608 | 37.935 | 23.440 | 1,714 | 1.1646 |
| 9 | 609 | 37.526 | 23.049 | 1,737 | 1.1717 |

T

Table 10

Average Cross Sections in the Second Dragon Capsule in Position E8 of the 30 MW Petten HFR Core

| Region | $\bar{\sigma}_D$ [4] $10^{-24}$ atoms/atom | $\bar{\sigma}_{Ni}$ mb | $\bar{\sigma}_{Fe}$ mb | $\bar{\sigma}_D \left(\frac{\hat{\sigma}(Ni)}{\bar{\sigma}(Ni)}\right)$ [4] $10^{-24}$ atoms/atom | $\left(\frac{\hat{\sigma}(Fe)}{\bar{\sigma}(Fe)}\right) / \left(\frac{\hat{\sigma}(Ni)}{\bar{\sigma}(Ni)}\right)$ |
|---|---|---|---|---|---|
| 1 | 584 | 28.423 | 16.653 | 2,199 | 1.2283 |
| 2 | 593 | 32.250 | 19.111 | 1,969 | 1.2144 |
| 3 | 588 | 32.982 | 20.377 | 1,909 | 1.1648 |
| 4 | 550 | 23.618 | 13.700 | 2,491 | 1.2406 |
| 5 | 578 | 32.912 | 19.976 | 1,879 | 1.1857 |
| 6 | 580 | 31.539 | 19.571 | 1,966 | 1.1597 |
| 7 | 554 | 38.605 | 25.129 | 1,537 | 1.1055 |
| 8 | 586 | 34.849 | 21.609 | 1,799 | 1.1605 |
| 9 | 581 | 30.779 | 18.842 | 2,020 | 1.1756 |

T

Table 11

Carbon-Atom Displacement Rate in Units of $10^{-24}$ Atoms/Atom
Normalised to Unit Equivalent Fission Flux

| Region | $\bar{\sigma}_D\left(\frac{\hat{\sigma}(Ni)}{\bar{\sigma}(Ni)}\right)$ | $\frac{\bar{\sigma}_D\left(\frac{\hat{\sigma}(Ni)}{\bar{\sigma}(Ni)}\right)}{\bar{\sigma}_D\left(\frac{\hat{\sigma}(Ni)}{\bar{\sigma}(Ni)}\right)}$ PLUTO |
|---|---|---|
| Normal Element in the Centre of the Dragon Core | 1,953 | 1.51 |
| First Ring of the DRAGON Core | 2,143 | 1.65 |
| Centre Rod of Uprated Element in Dragon | 1,687 | 1.30 |
| Outer Six Rods of Uprated Element in Dragon | 2,031 | 1.55 |
| 1st Dragon Capsule in Petten HFR Core 243 at 20 MW | 2,270 | 1.75 |
| 2nd Dragon Capsule in Petten HFR Core at 30 MW | 2,491 | 1.53 |
| Central Region of Petten HFR Core 243 | 1,721 | 1.33 |
| Empty Lattice Position PLUTO [4] | 1,299 | 1.00 |

given maximum dose of fast neutrons within the graphite. The maximum fast neutron dose recommended for AGR's is a Dido Nickel Dose of $2 \times 10^{22}$ n $cm^{-2}$ [10]. This maximum fast neutron dose is based on the requirement that the stored energy in the graphite should not be greater than 80% of the specific heat provided that the graphite temperature exceeds 315°C. Since the emphasis within the DRAGON PROJECT has now turned to the design of Low Enriched HTR's with similar cell geometries and moderator temperatures to that for AGR's, it was decided to calculate the time taken to reach this maximum fast neutron dose of $2 \times 10^{22}$ n $cm^{-2}$ within the graphite moderator for a typical design.

The details of the lattice cell were taken from [11] and are given below for completeness. The lattice chosen had a square pitch of 44.134 cm and a fuel radius of 13.2 cm with an access hole of 2.1 cm radius, the height of the reactor core was taken to be 400 cm, in addition the enrichment of the fuel was 3% and the mean power density in the reactor was 8 $MW/m^3$ or 46.73 MW/tonne U. Table 12 gives details of the composition in the different regions of the cell.

Table 12

Material Composition of Cell Regions

| Region | Isotope | No. of atoms x $10^{-24}/cm^3$ |
|---|---|---|
| Fuel | C | 0.0395 |
| | O | 0.11031625 |
| | U-235 | 0.0000474375 |
| | U-235 | 0.0015338125 |
| Moderator | C | 0.08525 |

## 3.2 Details of the Calculations

Only a single cell of the reactor was considered and the neutrons were reflected back into the walls of the cell to take account of neighbouring cells in the reactor. The source of fast neutrons was considered to be uniform throughout the fuel region. In order to reduce the length of time of the computer calculations the reactor was divided into two parts at the central plane and the neutron were reflected at this boundary to take account of those neutrons in the other half of the reactor. The cell was divided into 12 radial and 3 axial regions respectively, i.e., 36 regions in all, the outer boundary of the cell being square. The boundaries of the regions in the cell are given in Table 13.

Table 13

Boundaries of Regions in the Cell

| | | | | | | | | |
|---|---|---|---|---|---|---|---|---|
| Radius | cm | 2.1<br>17 | 13.2<br>18 | 14<br>22 | 14.5<br>22.067 | 15 | 15.5 | 16 |
| Axial height above the centre of the core | cm | 25 | 50 | 200 | | | | |

A total of 10,000 source neutrons were tracked in the cell to below 0.01 MeV and neutron spectra were calculated in each of the 36 regions in the cell. Details of the group structure of the neutron spectra are given in Table 5.

Using these spectra the programme calculated the Ni-58 (n,p) Co-58 reaction rate and the carbon atom displacement rate in graphite with the Thompson-Wright model for each region.

From these results the equivalent nickel fission flux $\phi_{fission}(Ni)$ defined by equation (1) was calculated for each region associated with 10,000 source neutrons. The number of source neutrons in the cell when the reactor was at 8 $MW/m^3$ was calculated and these values of $\phi_{fission}(Ni)$ were adjusted accordingly to give values corresponding to the reactor at this power. A further correction factor was applied to the nickel fluxes $\phi_{fission}(Ni)$, in order to convert them to the DIDO scale. To do this the carbon atom displacement rates in graphite were equated in this system to that in DIDO, so that from equation (7)

$$\phi_{DIDO}(Ni) = \frac{\bar{\sigma}_D\left(\frac{\hat{\sigma}(Ni)}{\bar{\sigma}(Ni)}\right)}{\left[\bar{\sigma}_D\left(\frac{\hat{\sigma}(Ni)}{\bar{\sigma}(Ni)}\right)\right]_{DIDO}} \phi_{fission}(Ni) \qquad (9)$$

Since the carbon atom displacement rate in DIDO is the same as that in PLUTO [4]:

$$\left[\sigma_D\left(\frac{\hat{\sigma}(Ni)}{\bar{\sigma}(Ni)}\right)\right]_{DIDO} = 1{,}299 \times 10^{-24} \text{ atoms/atom}$$

so that equation (9) becomes:

$$\phi_{DIDO}(Ni) = \frac{\bar{\sigma}_D\left(\frac{\hat{\sigma}(Ni)}{\bar{\sigma}(Ni)}\right)}{1{,}299} \phi_{fission}(Ni) \qquad (10)$$

Assuming the reactor operates at a uniform power level with a 75% load factor (i.e., 1 year = 300 days) then using equation (10) the number of years to reach a DIDO nickel dose of $2 \times 10^{22}$ n $cm^{-2}$ can be found. This has been done for the 12 radial regions in the first 25 cm above the central plane of the core and a list of the results are given in Table 14. Also the DIDO nickel dose after 1 year and the time taken to reach a DIDO nickel dose of $2 \times 10^{22}$ n $cm^{-2}$ for the regions in the cell are shown in Figs. 16 and 17.

### 3.3 Discussion

The results show that the minimum time to reach a DIDO nickel dose of $2 \times 10^{22}$ n $cm^{-2}$ in the moderator is 15.4 years in the region immediately adjacent to the fuel. This agrees well with the time of 14.3 years predicted by the fast neutron dose scale used for Calder Hall [10] which is 1,000 MWD/tonne of uranium is equivalent to $10^{20}$ n $cm^{-2}$ at the channel wall. Note that this definition for predicting nickel dose cannot be used for reactors with homogeneous cores, e.g., DRAGON or a Feed and Breed HTR system, since there is a much greater contribution to the fast neutron flux at the fuel moderator boundaries by the neighbouring fuel elements than in Calder Hall or an AGR. Nevertheless this definition will suffice for calculations of the nickel dose in the graphite immediately adjacent to the fuel in a low enrichment HTR with a lattice cell similar to an AGR. It is, therefore, not necessary to carry out Monte Carlo calculations to obtain the minimum graphite moderator residence time; Monte Carlo calculations need only to be made for obtaining a detailed knowledge of the relative build-up of carbon-atom displacement rate throughout the moderator.

From the calculations it can be seen that the fast neutron dose is a very steep function of distance from the outer fuel boundary and decreases by approximately a factor of two at the edge of the cell. This steep gradient will necessitate careful design of the moderator in order to avoid undue strains due to the relative shrinkage of the graphite by fast neutron damage.

## 4. CONCLUSIONS

The comparison of carbon-atom displacement in graphite in DRAGON and the Petten HFR has been achieved by calculating the fast neutron spectra in both reactors using a Monte Carlo method. From the calculations it was shown that the carbon-atom displacement rate per unit equivalent fission nickel flux in DRAGON and the Petten HFR were respectively 1.51 and 1.75 times that in PLUTO (or DIDO). Recent experimental results from DRAGON and the Petten HFR tend to confirm these ratios and give confidence in the calculations; however a direct experimental check of the calculations will be carried out.

Using the same method of fast neutron spectrum calculation in a typical Low Enrichment HTR with a power density of 8 $MW/m^3$ it was found that the time required to reach a DIDO nickel dose of $2 \times 10^{22}$ n $cm^{-2}$ in the graphite moderator immediately adjacent to the fuel was 15.4 years. The carbon atom

Table 14

Results of the Calculations in a Cell of a Low Enrichment HTR

| Radial Dimensions of Region | | $\int_{0.01\ \text{MeV}}^{14\ \text{MeV}} \phi(E)\,dE$ | $\bar{\sigma}_{Ni}$ | $\bar{\sigma}_D$ | $\bar{\sigma}_D \left(\frac{\hat{\sigma}(Ni)}{\bar{\sigma}(Ni)}\right)$ | $\frac{\bar{\sigma}_D \left(\frac{\hat{\sigma}(Ni)}{\bar{\sigma}(Ni)}\right)}{\left[\bar{\sigma}_D \left(\frac{\hat{\sigma}(Ni)}{\bar{\sigma}(Ni)}\right)\right]_{DIDO}}$ | DIDO Nickel Dose after 1 year | No. of Years to Reach a DIDO Nickel Dose of |
|---|---|---|---|---|---|---|---|---|
| Inner cm | Outer cm | | mb | $10^{-24}$ atoms/atom | $10^{-24}$ atoms/atom | | $\times 10^{-20}$ n cm$^{-2}$ | $2 \times 10^{22}$ n cm$^{-2}$ |
| 0 | 2.1 | 6.0001 | 39.173 | 555.26 | 1516.7 | 1.16759 | 15.7128 | 12.73 |
| 2.1 | 13.2 | 5.5695 | 35.689 | 554.25 | 1661.7 | 1.27921 | 14.5592 | 13.73 |
| 13.2 | 13.5 | 5.1285 | 30.457 | 538.09 | 1890.4 | 1.45527 | 13.0152 | 15.37 |
| 13.5 | 14.0 | 5.0281 | 27.502 | 523.70 | 2037.5 | 1.56851 | 12.4187 | 16.10 |
| 14.0 | 14.5 | 4.6841 | 25.414 | 520.04 | 2191.0 | 1.68668 | 11.4963 | 17.40 |
| 14.5 | 15.0 | 4.4976 | 24.440 | 518.81 | 2271.4 | 1.74857 | 11.0058 | 18.17 |
| 15.0 | 15.5 | 4.3330 | 21.982 | 514.38 | 2503.8 | 1.92748 | 10.5123 | 19.03 |
| 15.5 | 16.0 | 4.0996 | 22.489 | 511.10 | 2431.8 | 1.87206 | 9.8823 | 20.24 |
| 16.0 | 17.0 | 3.8985 | 21.428 | 505.84 | 2525.9 | 1.94450 | 9.3003 | 21.50 |
| 17.0 | 18.0 | 3.7061 | 22.094 | 494.32 | 2394.0 | 1.84296 | 8.6414 | 23.15 |
| 18.0 | 22.0 | 3.3314 | 18.526 | 476.89 | 2754.4 | 2.12040 | 7.4932 | 26.69 |
| 22.0 | 22.067 | 2.7510 | 16.762 | 459.07 | 2930.5 | 2.25597 | 5.9555 | 33.58 |

displacement rate per unit equivalent fission flux in the moderator was found to vary between 1.46 and 2.26 times that in PLUTO (or DIDO).

The calculations in this report now enable the DRAGON PROJECT to use the experimental results of the physical behaviour of graphite samples irradiated in DRAGON, and the Petten HFR in current designs of HTR's.

## 5. ACKNOWLEDGMENTS

The author wishes to express his gratitude to Dr. S. Wright, Mr. M. P. Ruffle at AERE Harwell for supplying the data for the calculations and advice in the use of SPECIFIC, and in addition to Dr. L. W. Graham for his constant interest in the work.

## 6. REFERENCES

[1] S. B. Wright, "Calculation of High Energy Neutron Spectra in Heterogenous Reactor Systems," AERE-R-4080.

[2] P. Carter, "Activation Cross Sections for the Reactions Fe-54 (n,p) Mn-54 and Fe-58 (n,$\gamma$) Fe-59 in Natural Iron." Conference on Radiation Measurements in Nuclear Power at Berkeley Nuclear Laboratories. 12th-16th September, 1966.

[3] L. Cranberg, et al., "Fission Neutron Spectrum of U-235," Phys. Rev. 103, No. 3, 662 (1956).

[4] M. W. Thompson, S. B. Wright, "A New Damage Function for Predicting the Effect of Reactor Irradiation of Graphite in Different Neutron Spectra." AERE-R-4701.

[5] E. P. Barrington, A. L. Pope, J. S. Story, "The Data in the Winfrith Nuclear Data Library. July, 1963." AEEW-R-4553.

[6] M. P. Ruffle, "SPECIFIC. A Monte Carlo Programme for High Energy Neutron Spectrum Estimation." AERE-R-4553.

[7] S. Francescon, "A Monte Carlo Programme for Calculating High Energy Spectra in Cylindrical Geometry in the IBM 709 Computer." AEEW-R-45.

[8] L. W. Graham, et al., "Graphite Irradiation Experiment in the DRAGON Reactor," D.P. Report 556.

[9] L. W. Graham, et al., "The Irradiation of Graphite in HFR Petten," D.P. Report 555.

[10] J. C. Bell, et al., "Stored Energy in the Graphite of Power Producing Reactors." Phil. Trans. Roy. Soc. London 254, 361, (1962).

[11] J. A. Macdougall. Dragon Internal Report.

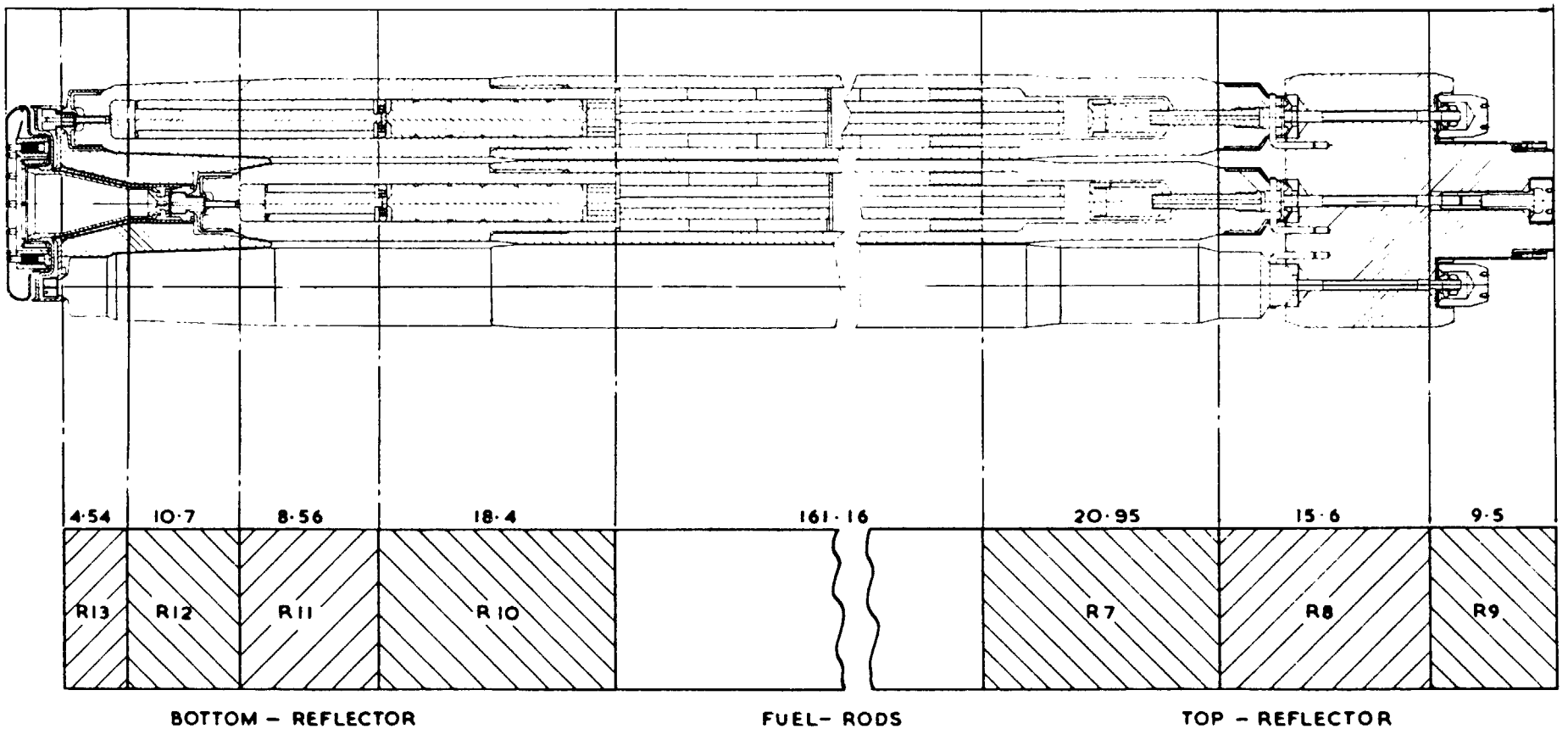


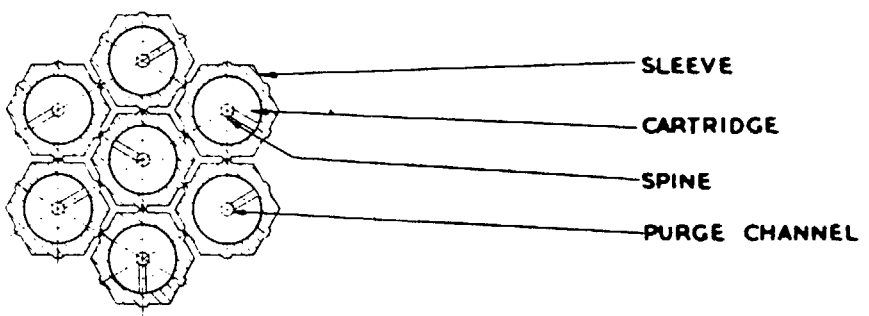


SECTION A-A

FIG. 1 THE DRAGON FUEL ELEMENT

CROSS-SECTION OF THE FUEL ELEMENT

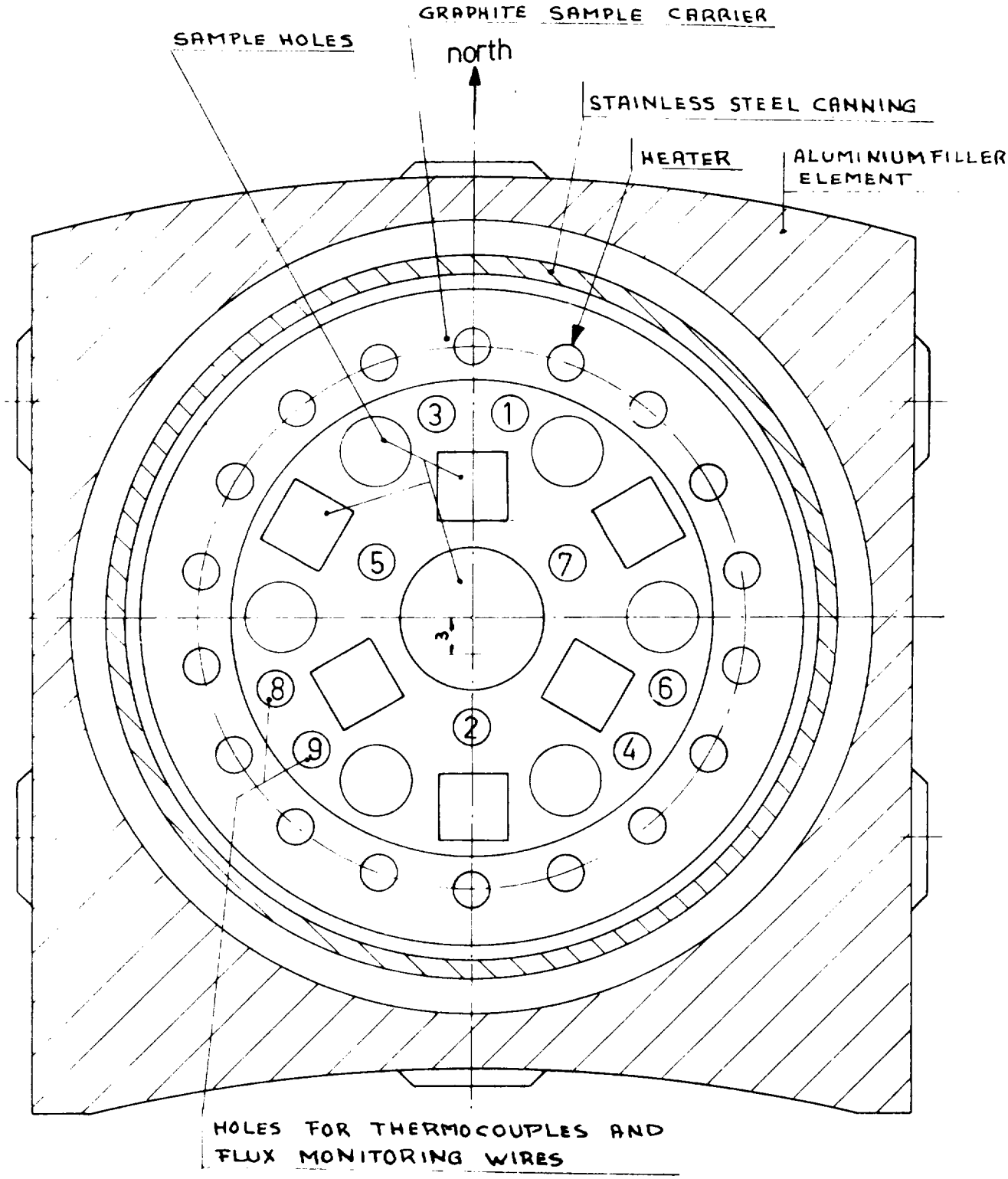


FIG. 2 CROSS SECTION OF A DRAGON CAPSULE IN THE PETTEN H.F.R.

fuel elements : 5096.59 grams $U^{235}$

control rods : 718.93 grams $U^{235}$

initial fuel charge: 5815.52 grams $U^{235}$

critical setting of control rods : 52.5 cm

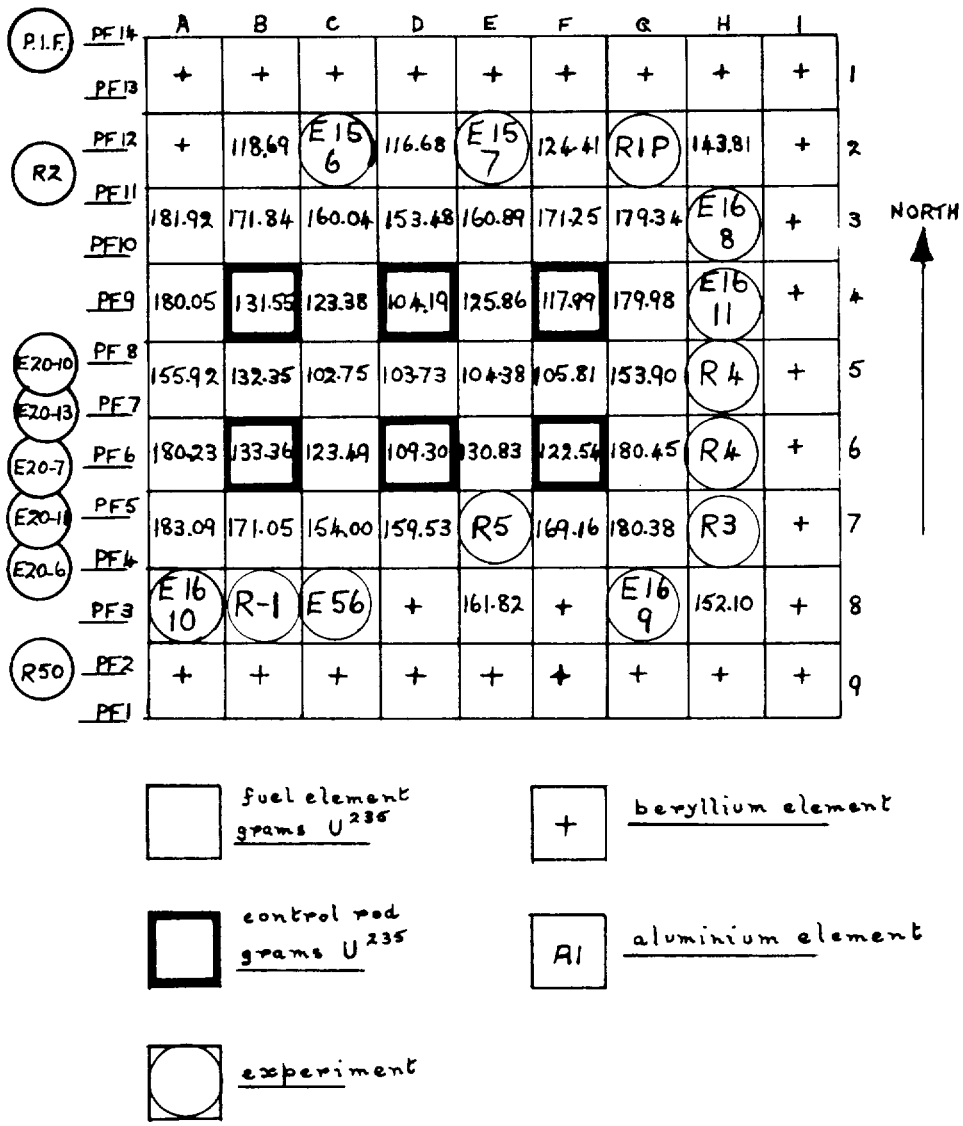


FIGURE 3. CROSS SECTION OF THE H.F.R. CORE 243

Total Uranium: 6163 g

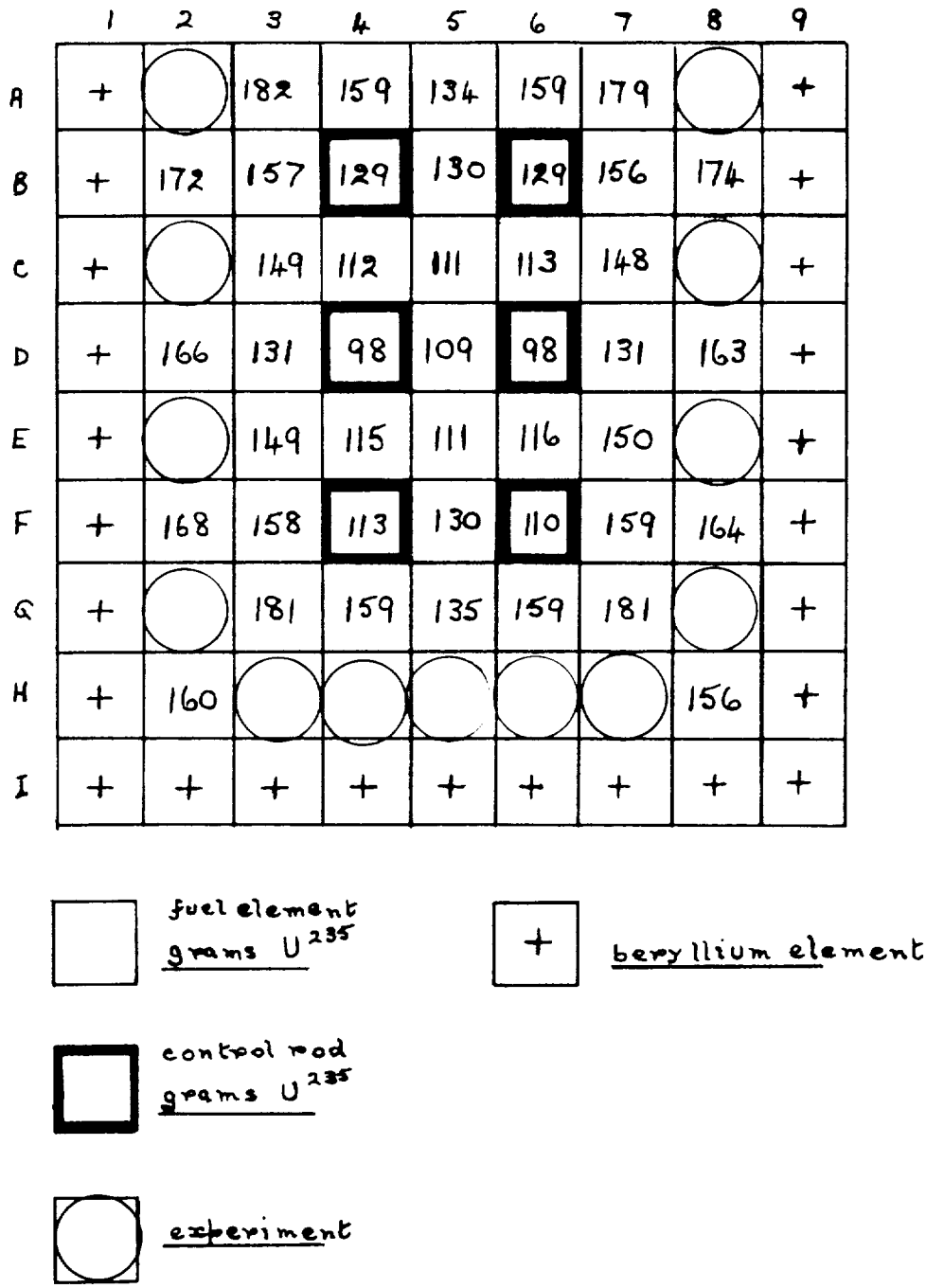


FIGURE 4. CROSS SECTION OF THE 30 MW CORE, H. F. R. PETTEN

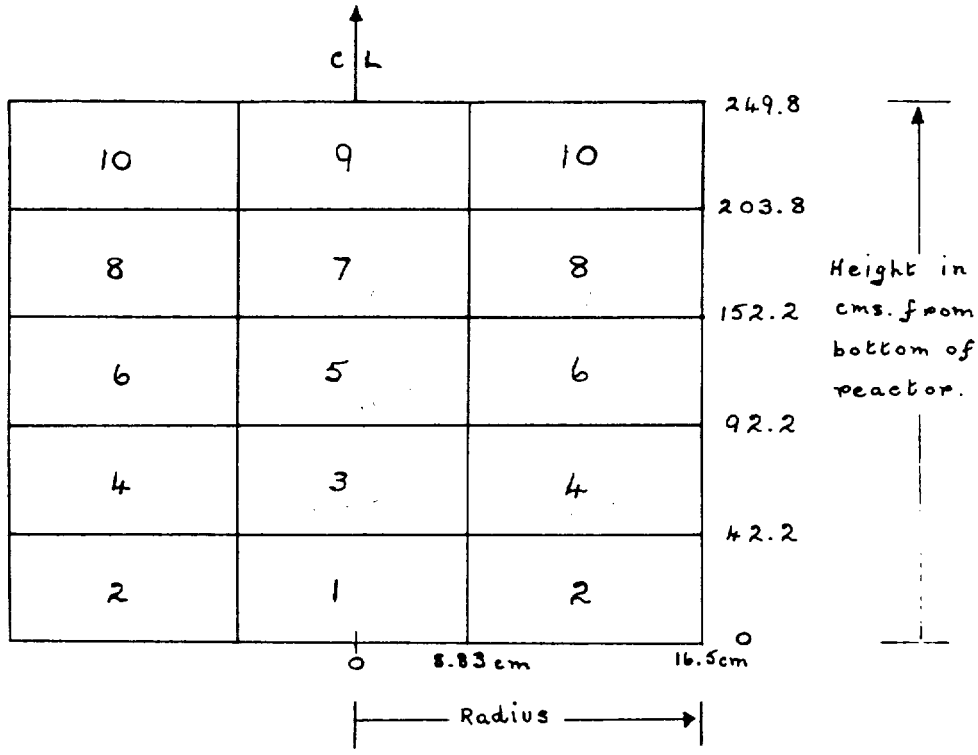


VERTICAL SECTION

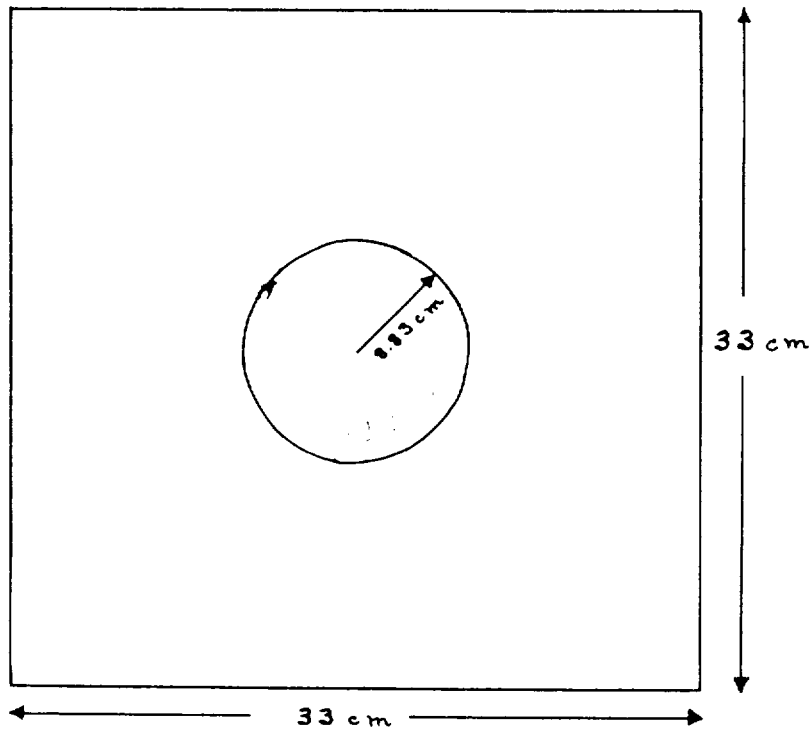


HORIZONTAL SECTION

FIGURE 5. Sections through the Dragon Reactor showing regions in which neutron spectra were calculated.

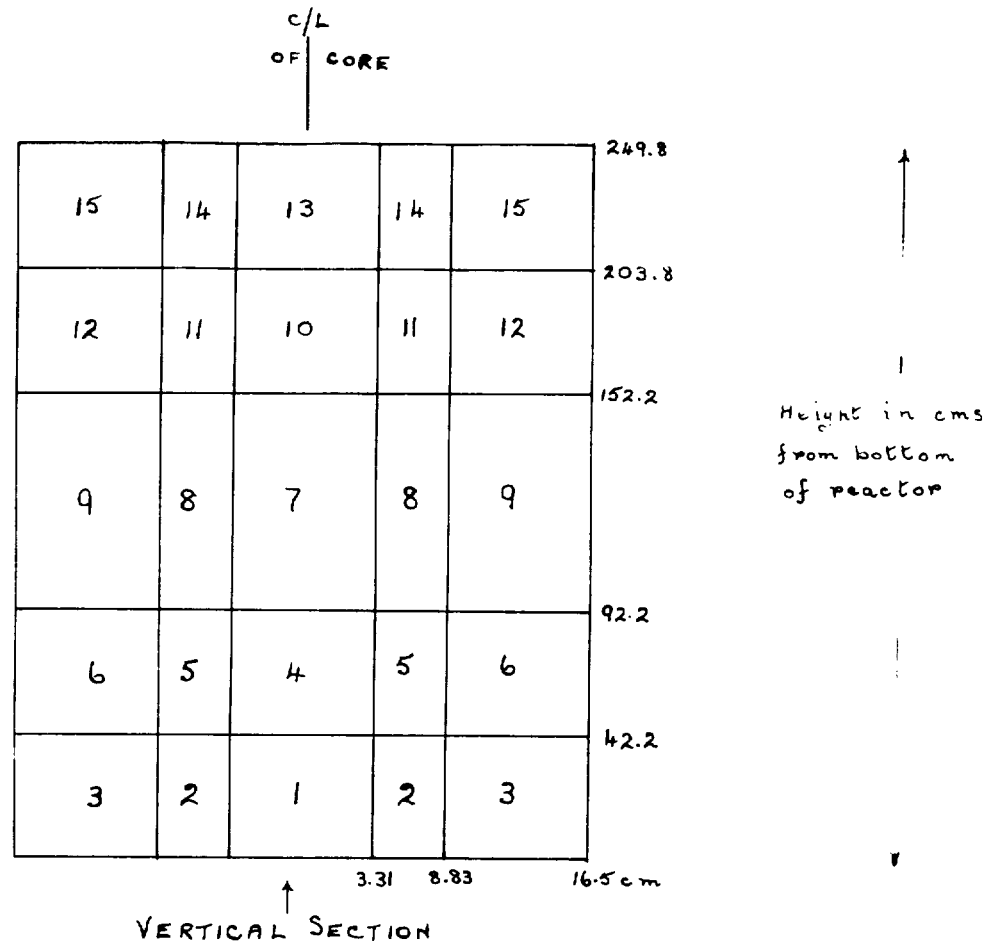


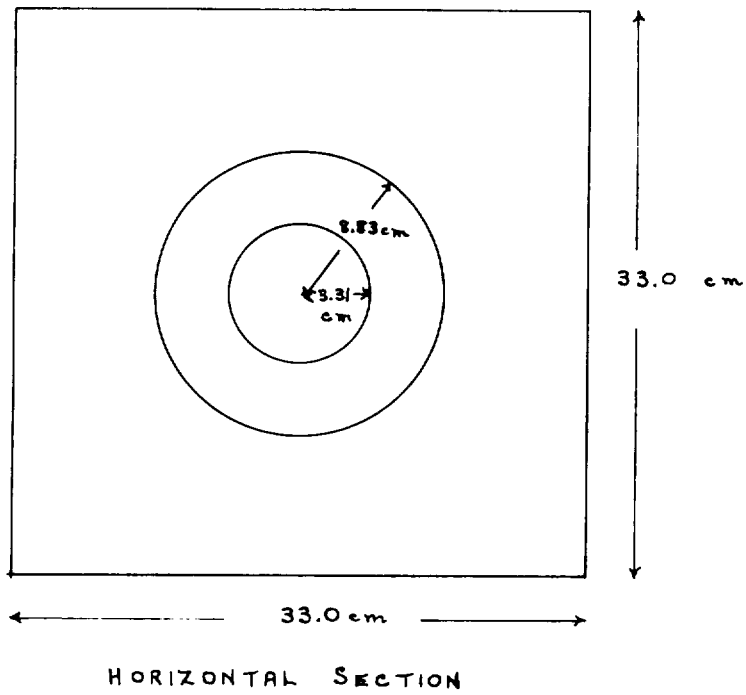


FIGURE 6. REGIONS IN WHICH SPECTRA CALCULATIONS WERE PERFORMED ON THE UPRATED UZR ELEMENT IN DRAGON.

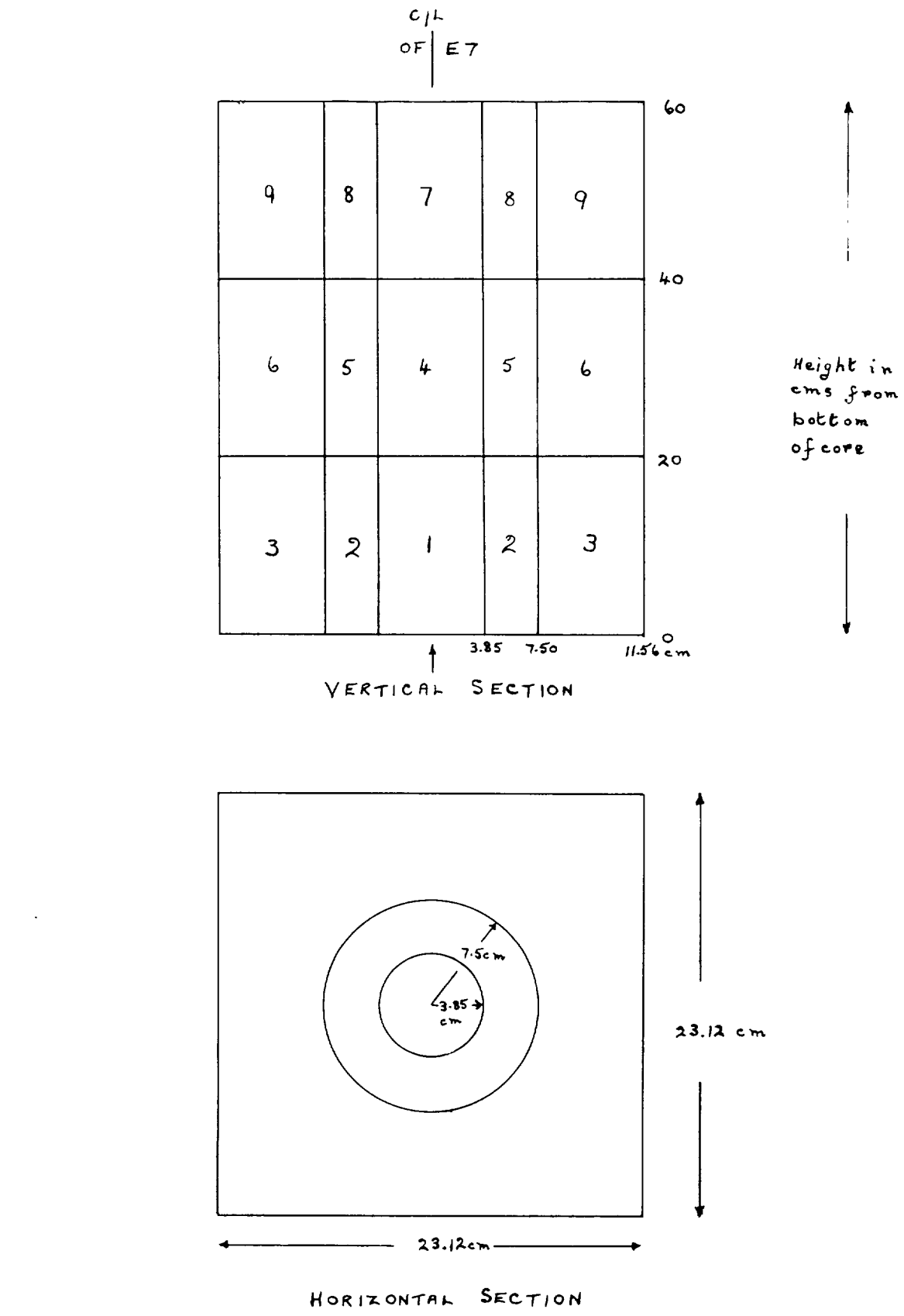


FIGURE 7. REGIONS IN WHICH SPECTRA CALCULATIONS WERE PERFORMED IN E7 OF THE H.F.R. CORE 243

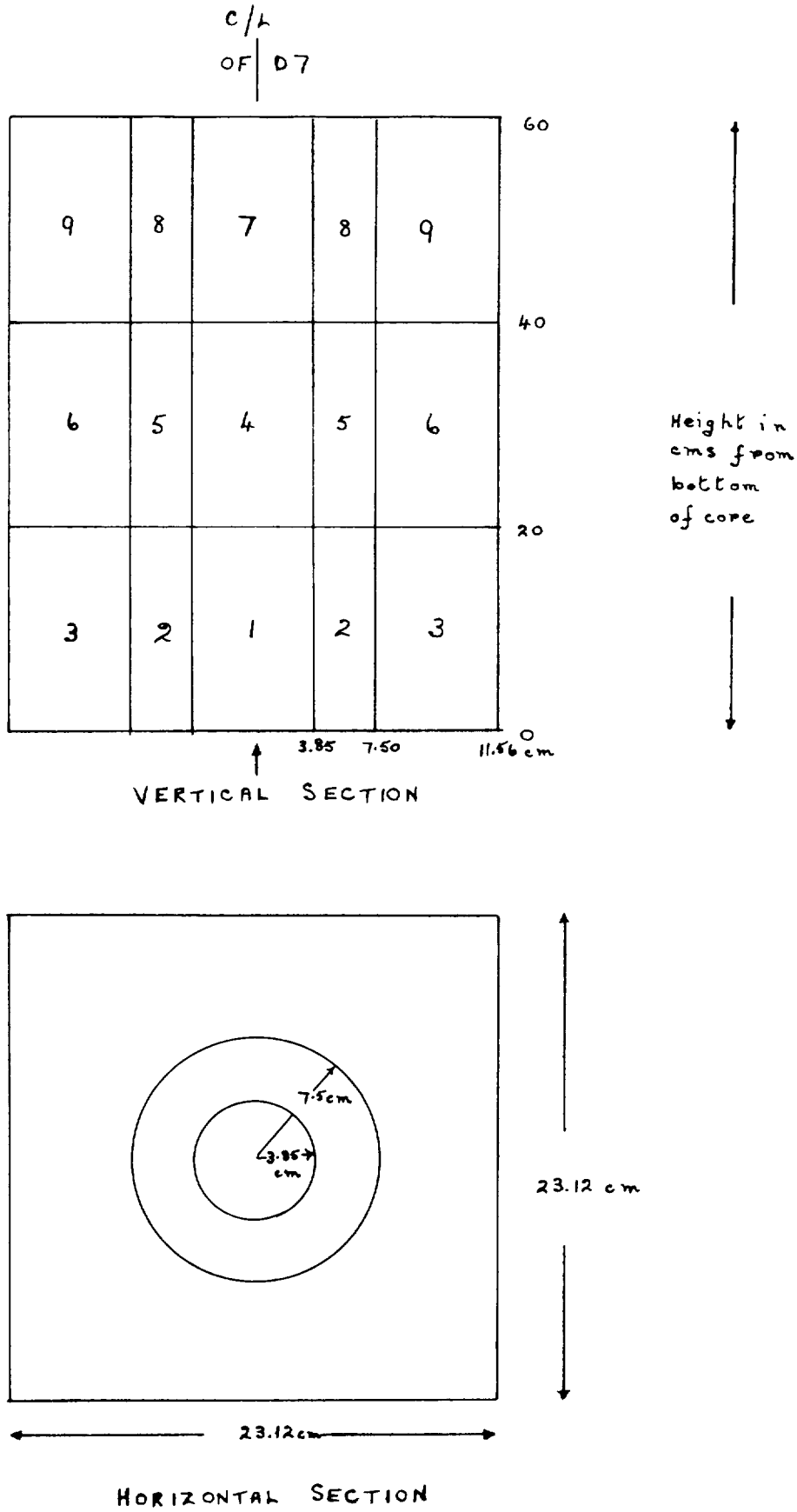


FIGURE 8. REGIONS IN WHICH SPECTRA CALCULATIONS WERE PERFORMED IN D5 OF THE HFR CORE 243

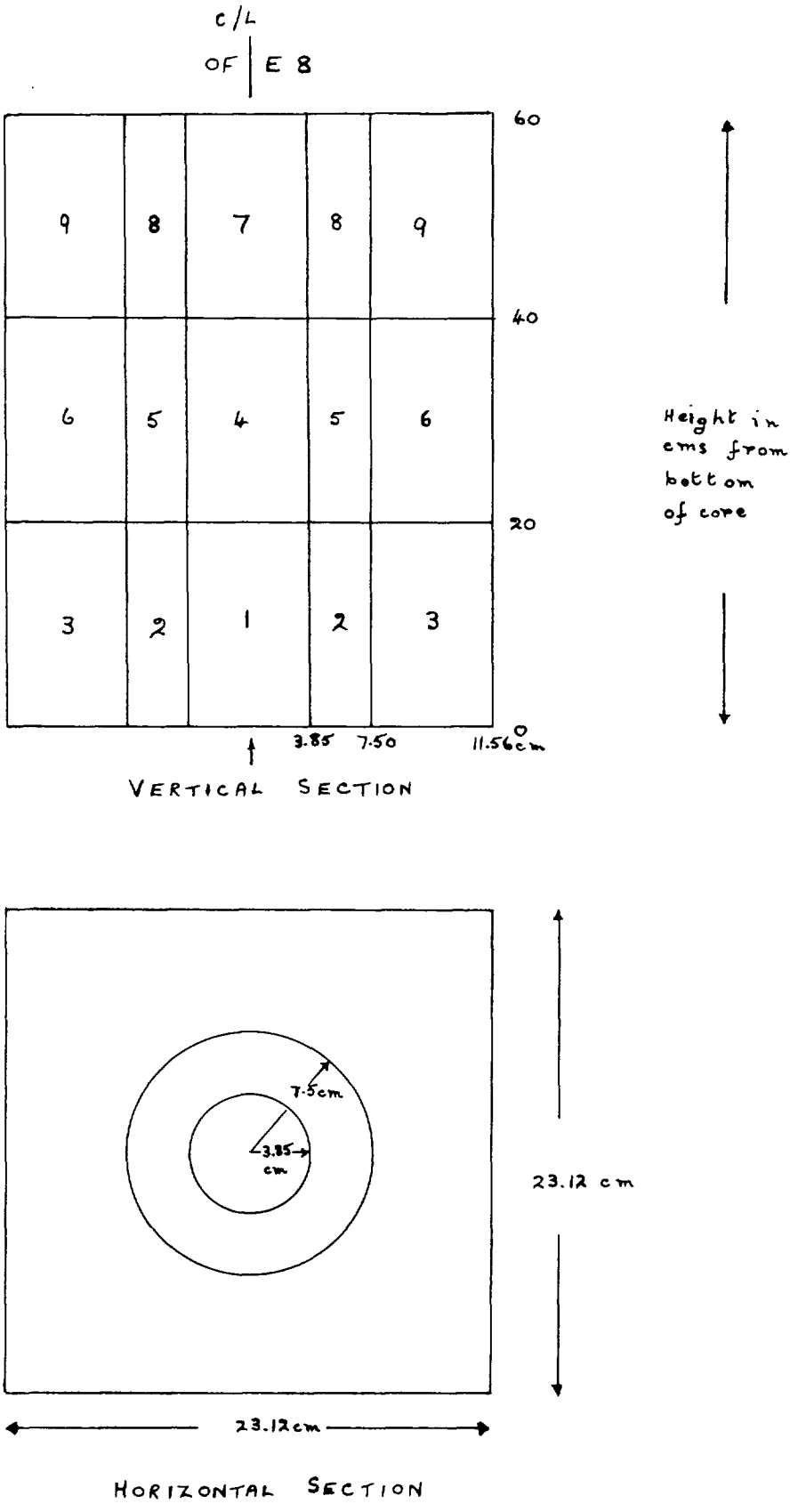


FIGURE 9. REGIONS IN WHICH SPECTRA CALCULATIONS WERE PERFORMED IN E 8 OF THE 30 MW HFR CORE

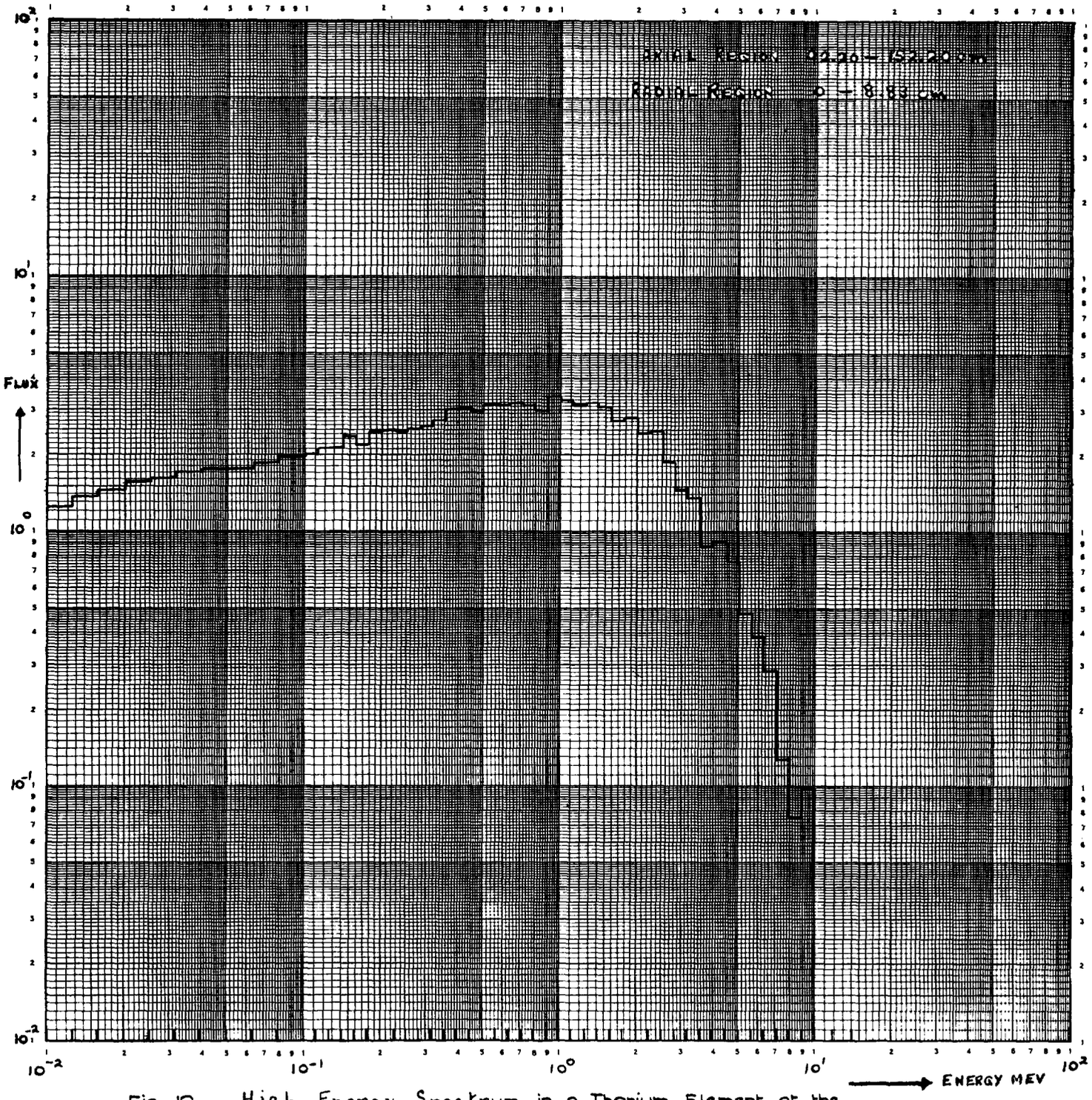


Fig. 10 High Energy Spectrum in a Thorium Element at the Centre of the First Dragon Core.

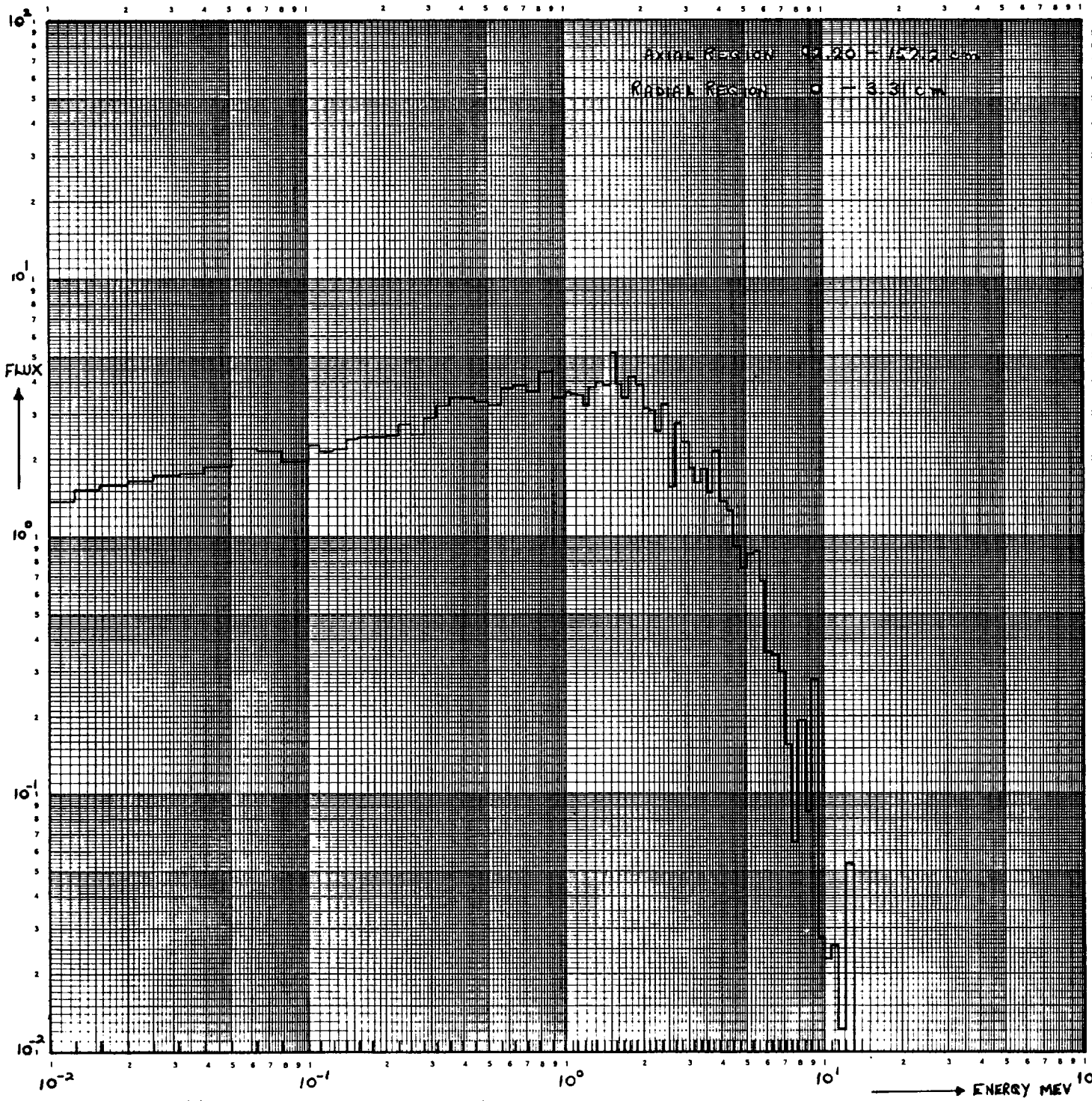


Fig. 11 High Energy Spectrum in the Central Fuel Rod Dragon Uprated ZRU Element

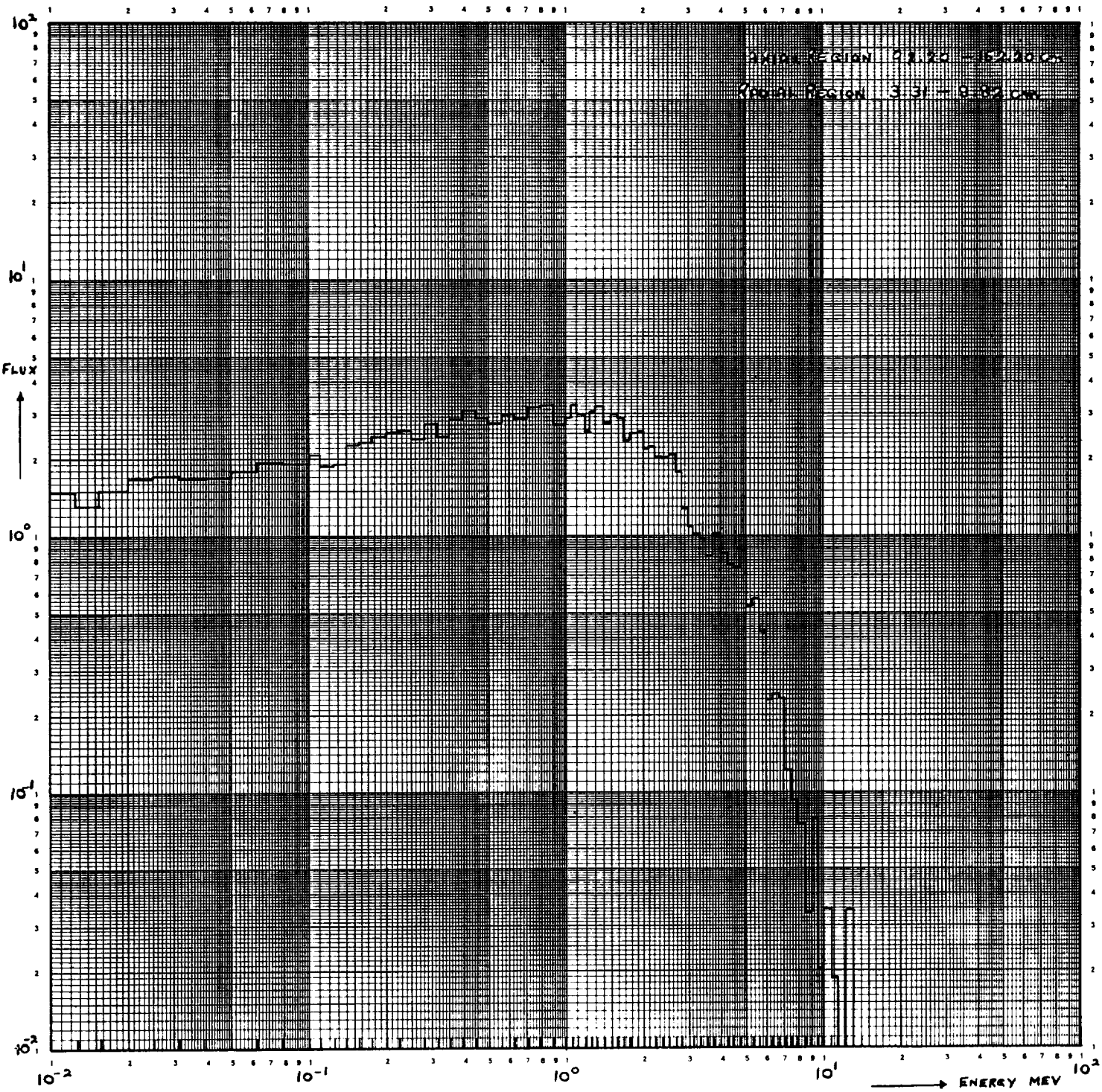


Fig. 12 High Energy Spectrum in the Outer Six Fuel Rods of the Dragon Uprated ZRU Element

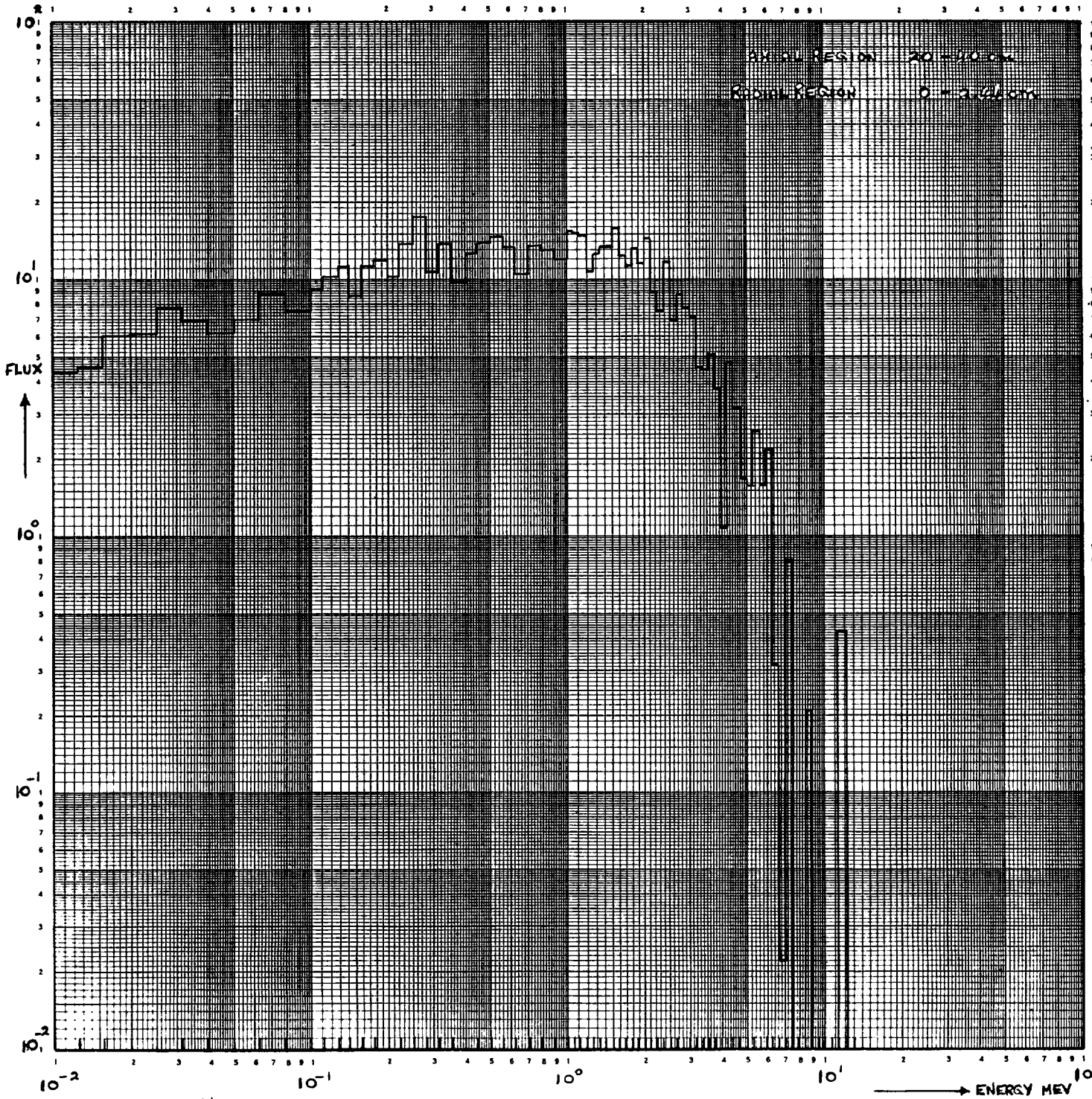


Fig. 13 High Energy Spectrum in the First Dragon Capsule of the Petten H.F.R.

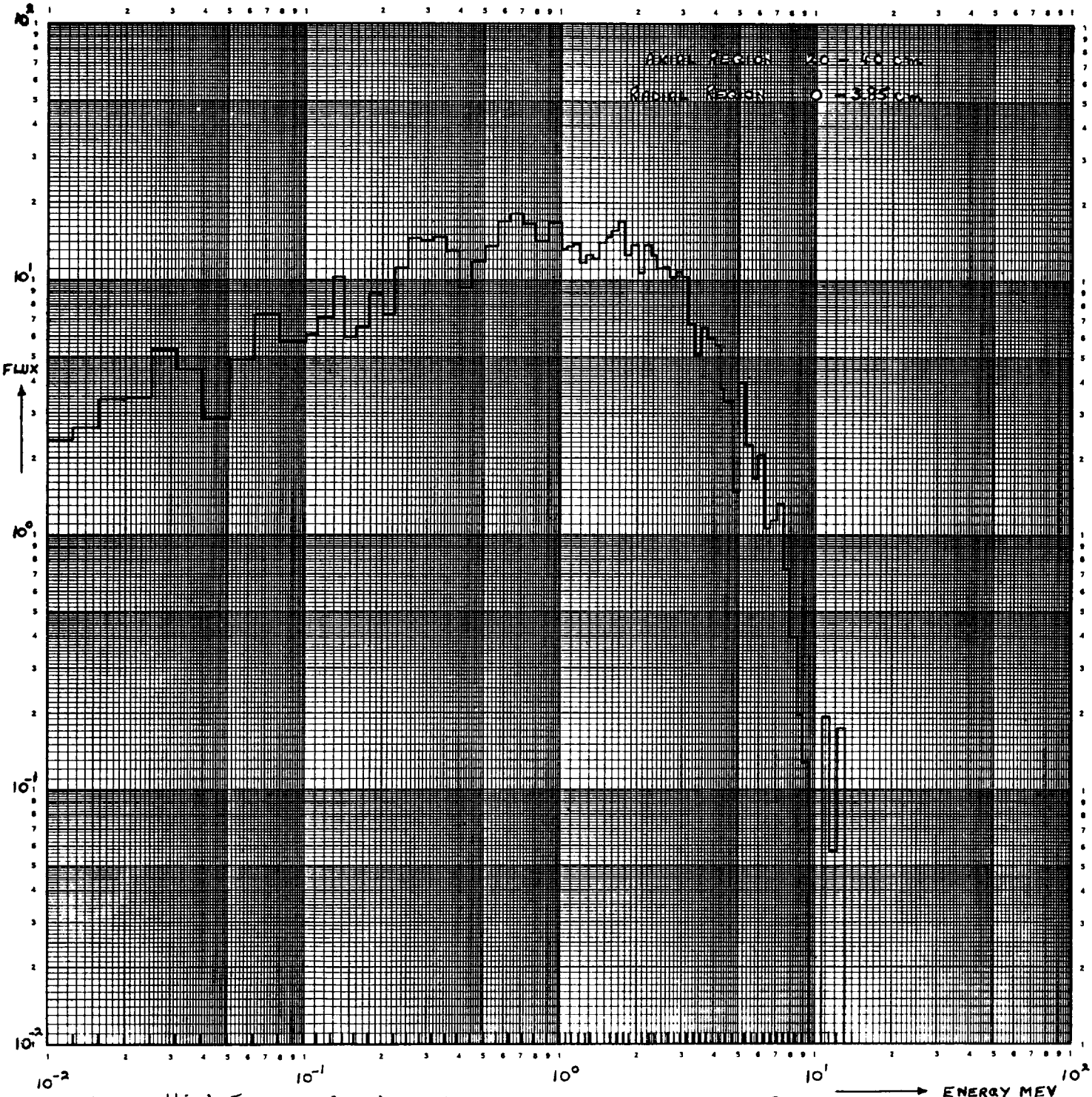


Fig. 14 High Energy Spectrum in D5 of the Petten H.F.R. Core 243

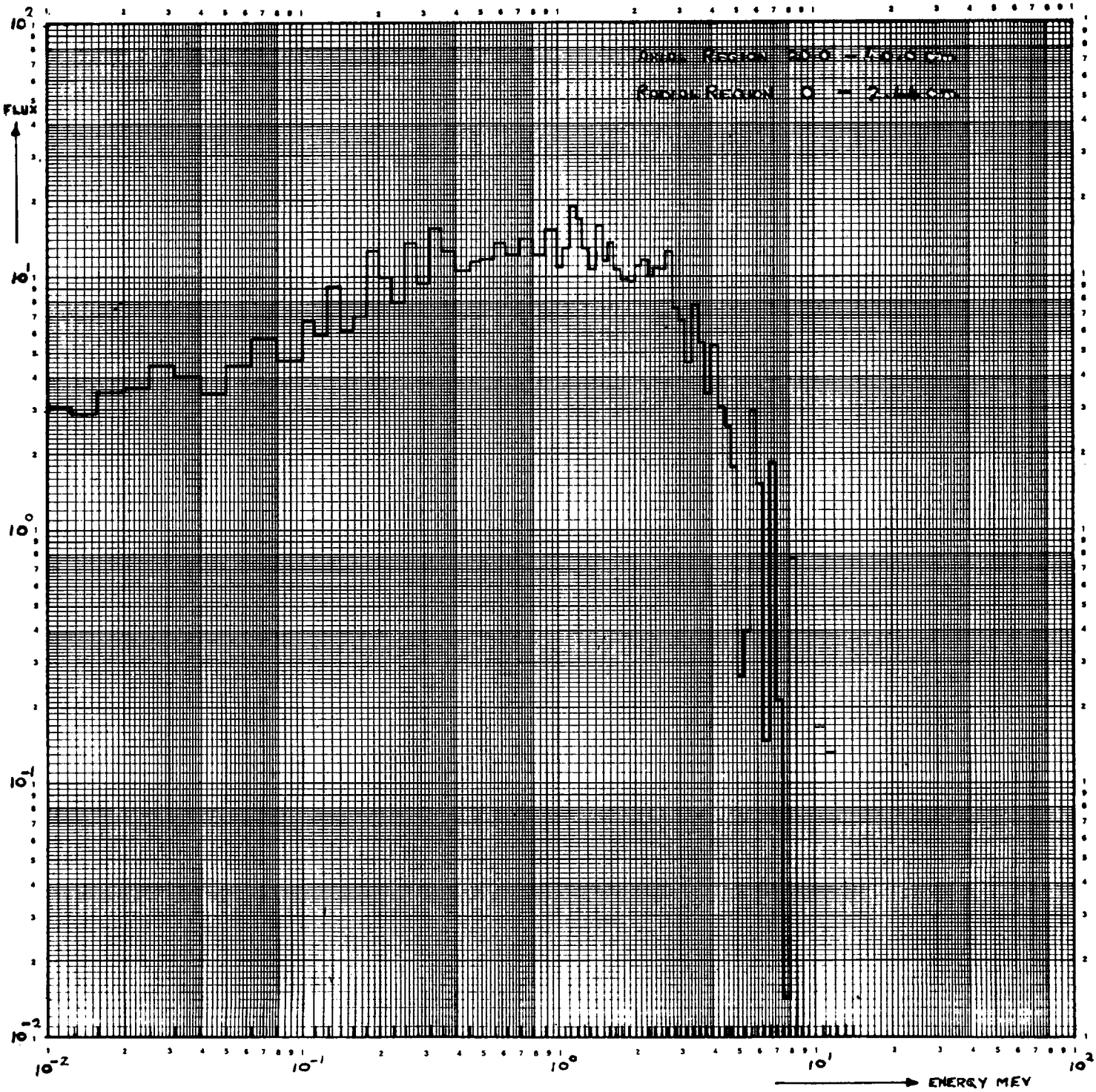


FIG. 15 High Energy Spectrum in Second Dragon Capsule in the Petten H.F.R.

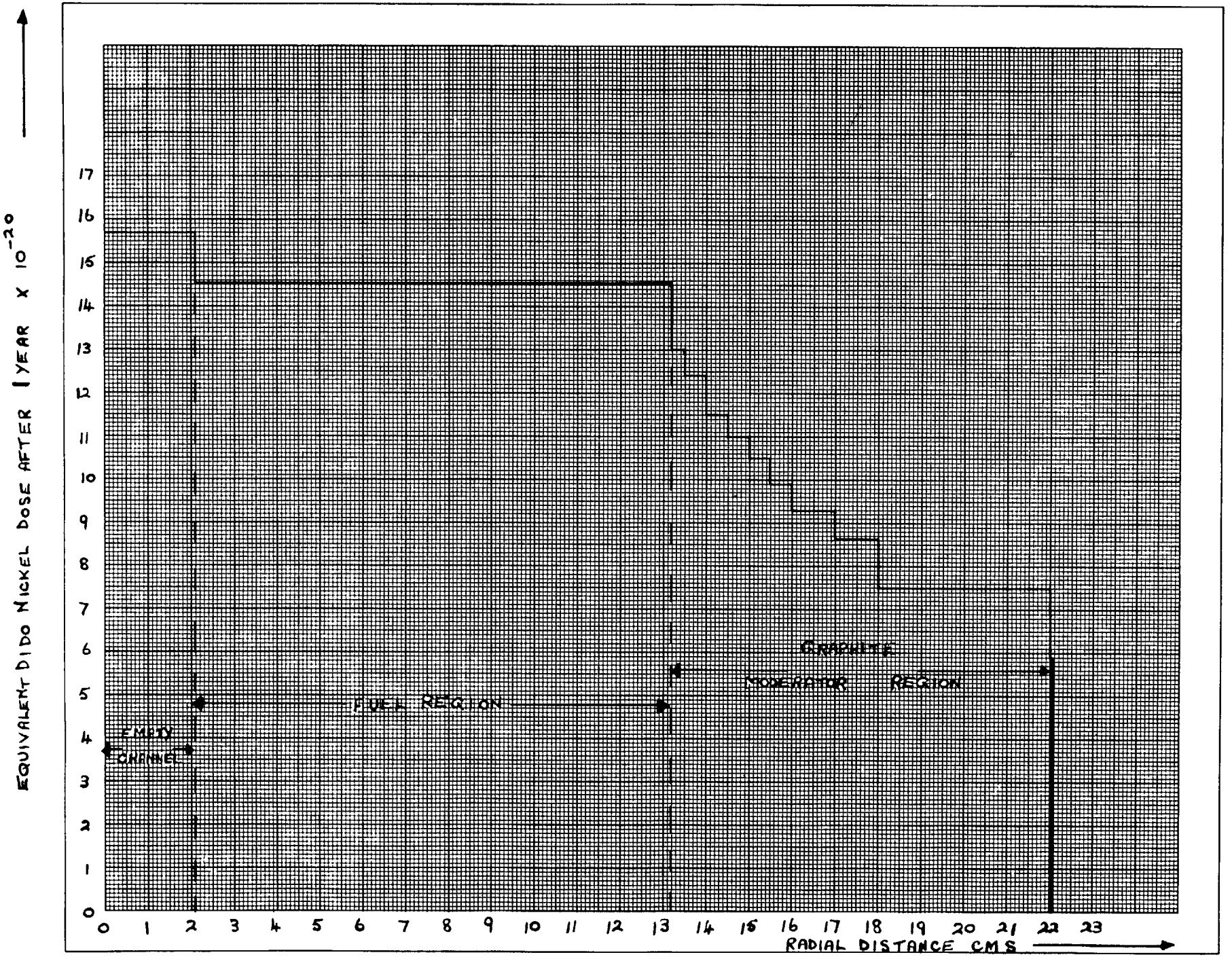


FIGURE 16. THE DIDO NICKEL DOSE IN A CELL OF A LOW ENRICHED HTR SYSTEM.

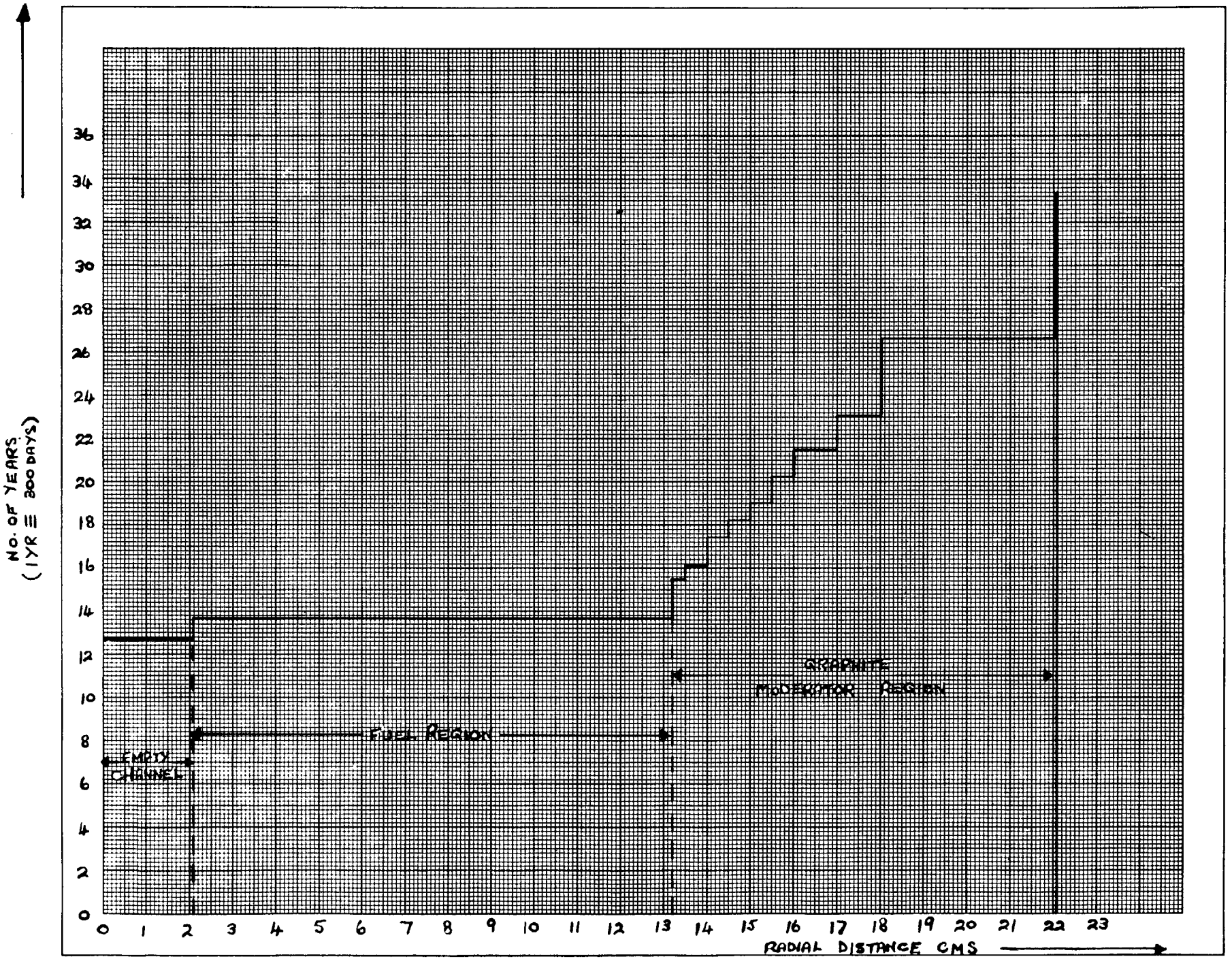


FIGURE 17. THE NUMBER OF YEARS REQUIRED TO REACH AN EQUIVALENT DIDO NICKEL DOSE OF $2 \times 10^{22}$ IN A CELL OF A LOW ENRICHED HTR.